MICROTURBINE MATERIALS PROGRAM

Annual Progress Report for
FY 1999

Prepared by:

David P. Stinton, ORNL Program Manager
Michael A. Karnitz, Mgr. Industrial Technologies Programs
Oak Ridge National Laboratory

For:

Department of Energy
Office of Industrial Technologies
Energy Efficiency and Renewable Energy

MICROTURBINE MATERIALS PROGRAM

July – September 1999

TABLE OF CONTENTS

CERAMICS LIFE PREDICTION

Ceramics Life Prediction Coordination

A. A. Wereszczak

Oak Ridge National Laboratory, Oak Ridge, Tennessee

NDE Technology Development for Microturbines

W. A. Ellingson and H. R. Lee

Argonne National Laboratory

Life-Prediction of Toughened Ceramics

N. Nemeth

NASA, Glenn Research Center, Cleveland, OH

Assessment of Recuperators for Microturbines

Ogbemi O. Omatete, Oak Ridge National Laboratory

Objective

Current microturbines utilize primary surface recuperators that operate at temperatures of about 600°C to boost their efficiency to ~30% LHV. Advanced microturbines being developed to obtain greater than 40% efficiency will likely require recuperators that operate at higher temperatures (650 to 900°C). The objective of this project is to assess the availability of metallic or possibly ceramic recuperators that could safely operate at temperatures up to 900°C.

Highlights

The assessment indicated that there were no ceramic recuperators for microturbines in current production. Most of the research in the area of ceramic recuperators in the United States had been abandoned more than ten years ago at the end of the "energy crisis." AlliedSignal Composites, Inc. (Lanxide) is developing a thin-sheet, ceramic recuperator based on alumina (Al_2O_3) particulates in an Al_2O_3 matrix that will be tested at RPI in the coming months. The European (AGATA) and Japanese (CGT 300) projects were developing ceramic recuperators, but their efforts have been scaled down. Most U. S. microturbine manufacturers are more interested in metallic recuperators for their immediate production plans. They give the impression that the need for ceramic recuperators is five years to a decade hence. The primary surface recuperator (PSR) seems to have been selected by most manufacturers, although there is a concern about cost and capacity to meet the demand. Current microturbines attain ~30% efficiency by using PSR fabricated with Type 347 stainless steel and operate at gas inlet temperatures of <650°C. To increase their efficiency to the >40% goal of the Office of Industrial Technology (OIT) Advanced Microturbine Technology Program would require a concomitant increase in recuperator materials temperature limit. Research to extend the temperature limit of current materials and/or select new alloys is in progress. However, research on ceramic recuperators needs to be resuscitated if they will be needed in the next decade.

Technical Progress

This assessment involved literature review and communication with those who have worked or are working in the area of recuperators. The assessment did not involve technical research. As mentioned in the highlights, only a few companies or institutions are working on ceramic recuperators at this time. There is a major U.S. company, Solar Turbines, Inc., that is involved in the production of the primary surface metallic recuperators used on several commercial microturbines. There appears to be a concern by the microturbine manufacturers about the cost and the ability to meet demand. A draft report, "Assessment of Recuperators for Microturbines," by O. O. Omatete, P. J. Maziasz, and D. P. Stinton was completed and is under review.

Status of Milestones

The final report on the assessment is in preparation. A workshop on recuperators for microturbines is being planned for late May, 2000, in Denver, Colorado.

Industry Interactions

This assessment has involved visiting and communicating with companies in the microturbine industry. Both AlliedSignal Power Systems, Inc., Torrance, California and Capstone Turbine Corporation, Tarzana, California were visited to discuss their recuperator needs. After attending an International Colloquium and Exhibit on Environmentally Preferred Advanced Energy Generation (ICEPAG) at Irvine, California in March 1999, a visit was made to the University of California at Irvine where testing of the microturbines is ongoing. At the Power Gen Conference in Orlando, Florida in December 1998, and at the ASME – Intl. Gas Turbine & Aerospace Congress in Indianapolis, Indiana, we saw exhibits of microturbines and interacted with the manufacturers.

Problems Encountered

None.

Publications

Omatete, O. O., Maziasz, P. J., & Stinton, D. P., "Overview of Recuperator Issues for Advance Microturbine Technology," 44th ASME Technical Congress & Gas Turbine Users Symposium, Indianapolis, IN, June 1999. Viewgraphs of presentation sent to 30 participants.

Omatete, O. O., Pint, B. A., and Stinton, D. P., "Materials Requirements for Advanced Microturbine Recuperators," Abstract, 2000 IGT Conference, Germany.

Materials Selection for High Temperature Metallic Recuperators for Improved Efficiency Microturbines

B. A. Pint , R. W. Swindeman, P. F. Tortorelli and K. L. More, Oak Ridge National Laboratory

Objective

The goal of this work is to employ laboratory testing of foil material (~100µm or 4 mil thickness) to select alloys for higher temperature (750-1000°C, 1400-1800°F) recuperator performance based primarily on corrosion resistance. Ultimately, a maximum operating temperature for each alloy will be determined. An additional component is to characterize current-technology recuperators operated at higher temperatures (e.g., 700°C) to assess failure modes. This project complements additional work at ORNL on the development of optimized processing of advanced alloy foils for creep resistant microstructures.

Highlights

This project began in July 1999, and initial steps have been taken to set up a test matrix for the coming year. Five alloys have been selected for initial characterization: three chromia-forming alloys: (1) 321 stainless steel, (2) NF709, a 20/25/Nb stainless steel and (3) Inconel 625; and two alumina forming alloys: (4) Haynes 214 and (5) PM2000, a mechanically alloyed, oxide-dispersion strengthened FeCrAl alloy. In each case, foil (~100µm or 4 mil) fabrication has begun or material has been ordered from manufacturers. Two new furnaces equipped for water vapor corrosion testing at 750-1000°C are under construction and will be complete by the end of October.

Technical Progress

Foil has been fabricated from the first three materials: 321 stainless steel, NF709, and Inconel 625. Creep and corrosion testing is just beginning on foil materials. No data is available at this time.

TEM specimens are being prepared on PM2000 oxidized for 100, 1h cycles at 1100°C with and without water vapor in the oxidation environment. Specimens of Haynes 214 are being oxidized under similar conditions for TEM analysis, as are specimens of 321 for 100h at 700°C. The goal of this work is to look for a microstructural explanation for the deleterious role of water vapor on oxidative lifetime.

Status of Milestones

Work is proceeding on five alloys to meet the objectives of this program.

Industry Interactions

August meeting at ORNL with AlliedSignal. General discussions were held.

Contacted J. Preston Montague at Solar Turbines, Inc., to ask about field-exposed specimens for characterization.

Problems Encountered

None.

Publications
None.

CREEP BEHAVIOR OF ADVANCED ALLOYS FOR MICROTURBINE RECUPERATORS

P.J. Maziasz and R.W. Swindeman, Oak Ridge National Laboratory

Objective

This program is focused on evaluating foils of high-temperature, austenitic, stainless steels, stainless alloys, and superalloys for compact recuperator applications for advanced microturbines. Compact primary surface recuperators (PSRs) for current and advanced land-based, gas turbine engines are made from Type 347 stainless steel foil and are limited to temperatures of 660°C and below. Combinations of oxidation and corrosion behavior and tensile and creep strength determine the upper temperature and useful lifetime limits. Microturbines will require PSRs capable of prolonged use at higher temperatures. For exhaust gas temperature above 900°C, structural ceramics may well be necessary, but at temperatures of 700-850°C there are a number of stronger and more corrosion-resistance stainless steels, stainless alloys, and superalloys that should be considered and evaluated for cost-effective performance as foils relative to Type 347 stainless steel. While properties behavior of these alloys is generally known for processing and fabrication into other high-temperature components (i.e., heat-exchanger piping, gas turbine components), there is little or no information on these alloys fabricated into the 0.003 - 0.004-in-thick foils used for PSRs. Foils with very fine grain sizes tend to have less creep resistance relative to coarse-grained products of the same alloy, unless the alloy composition and/or processing are adjusted. Therefore, the initial phase of this project is to produce and evaluate foils of a wide range of commercially available alloys then down select the alloys most suitable for further improvement and optimization. This project complements additional work at ORNL on the selection of materials with improved corrosion/oxidation resistance at temperatures ranging from 700 to 850EC.

Highlights

Lab-scale processing of Type 347 stainless steel has produced improvements in the creep-resistance at temperatures of 650-700°C for advanced turbine system (ATS) compact recuperator applications. This success was achieved by a Solar Turbines/Allegheny-Ludlum/ORNL team and is being tested on a commercial-scale production level. For the higher temperatures required for advanced microturbines (up to 900°C and above), PSRs will need to be made from stainless steel alloys or superalloys that can withstand oxidation and corrosion attack as well as resist creep conditions. This program is currently producing foils and will creep-test a range of stronger, more corrosion-resistant Fe- and Ni-based alloys in lab-air at temperatures of 750-850°C. Commercially produced stainless steel alloys have been obtained and are being processed into fine-grained foils to measure their creep-resistance relative to standard Type 347 stainless steel. Microstructural analysis will reveal the strengthening mechanisms in such foils and provide the information necessary to help down select and optimize the processing of the best alloys.

Technical Progress

A group of high-temperature stainless steel alloys and superalloys were identified on the basis of having more Cr (or Cr+Al) than Type 347 stainless steels for oxidation resistance and better high-temperature strength and creep resistance for the initial evaluation and selection round (Table 1). Generally, high-temperature strength and creep resistance is based on solid-solution or precipitation-strengthening roles of the various alloying elements. Precipitate strengthening is usually derived either from finely distributed carbide or from ordered γ' second-phase particles. Of particular concern in this study is how fabrication into fine-grained, 0.003-0.004-in-thick foil affects these native, microstructural, strengthening mechanisms especially during lower-stress, long-term creep. All of the alloys listed in Table 1 have been obtained and are being processed into foils at ORNL. Creep testing and characterization of as-fabricated microstructures will begin next quarter. Alloys noted as "developmental" in Table 1 have generic compositions of the base alloys given with other details being labeled as not available (n.a.) at the present time due to CRADA restrictions and other considerations.

Table 1 - Compositions of Potential Advanced Austenitic Stainless Alloys for Microturbine Recuperator Applications (wt.%)

Alloy/Vendor	Fe	Cr	Ni	Co	Mo	Nb	W	C	Si	Ti	Al
347 steel/ 0.003 Allegheny-Ludlum		68.7	18.3	11.2	0.2	0.3	0.64	-	0.03	0.6	0.001
mod. 20-25Nb/ Allegheny-Ludlum (developmental)	53	20	25	-	1.5	0.3	-	n.a.	n.a.	n.a	n.a.
mod. 803/ INCO (developmental)	40	25	35	-	n.a.	n.a.	-	0.05	n.a.	n.a.	n.a.
Thermie alloy/ (INCO)	2.0	24	48	20	0.5	2.0	-	0.1	0.5	2.0	0.8
alloy120/ 0.1 (Haynes)		33	25	32.3	3 max	2.5 max	0.7	2.5 max	0.05 (+ 0.2 N)	0.6	0.1
alloy 214 (Haynes)	3.0/	16	76.5	-	-	-	-	-	- (+ minor Y)	-	4.5
alloy 230 (Haynes)	3.0 max/	22	52.7	5 max	2	-	14	0.1	0.4 (+ trace La)	-	0.3
alloy 625/ (INCO)	3.2	22.2	61.2	-	9.1	3.6	-	0.02	0.2	0.23	0.16

Status of Milestones

New project.

Industry Interactions

Formal interactions exist between ORNL and several industry partners through CRADAs related to this project, including CRADAX95-0453 with Solar Turbines, Inc.. and CRADAX98-0529 with INCO Alloys International, Inc. Informal interactions to obtain alloys to make into foils were also established with these companies and with Allegheny-Ludlum and Haynes Alloys International. It is expected that contact will also be made with microturbine recuperator end-users through Solar Turbine, Inc., who manufactures and supplies such products.

Problems Encountered

None.

Publications

P.J. Maziasz, R.W. Swindeman, (ORNL), J.P Montague, M. Fitzpatrick, P.F. Browning (Solar

Turbines, Inc.), and J.F. Grubb, R.C. Klug, R.A. Painter (Allegheny-Ludlum), "Stainless Steel Foil with Improved Creep-Resistance for Use in Primary Surface Recuperators for Gas Turbine Engines," Conf. Proc., Gas Turbine Materials Technology, eds. P.J. Maziasz, I.G. Wright, W.J. Brindley, J. Stringer, and C. O'Brien, ASM-International, Materials Park, OH (1999) pp. 70-78.

P.J. Maziasz, R.W. Swindeman, J.P. Montague, M. Fitzpatrick, P.F. Browning, J.F. Grubb, and R.C. Klug, "Improved Creep-Resistance of Austenitic Stainless Steel for Compact Gas Turbine Recuperators," to be published in Proc., 13th Annual Conference on Fossil Energy Materials, May 11-13, 1999, Knoxville, TN, Oak Ridge National Laboratory Report.

Development of Silicon Nitride Ceramic Materials with Elongated Grain Microstructures Exhibiting High Fracture Toughness

Jim Wimmer, AlliedSignal Ceramic Components, and Chien-Wei Li, AlliedSignal Research and Technology

Objective

Demonstrate the reproducibility of gelcast and slipcast AS800 mechanical properties in a production environment, characterize and improve the AS800 fabrication process to improve strength and oxidation resistance, demonstrate the ability to gelcast and densify thick sections required for lower-cost, integral gas turbine rotors, and design a ceramic, radial rotor for microturbine application.

Highlights

Processing and testing multiple batches over an 18-month period have demonstrated the consistency of the mechanical properties of slipcast and gelcast AS800 silicon nitride.

A new coating system is being evaluated to prevent the recession of silicon nitride airfoils in the high temperature, high moisture, combustion environment typical of gas turbine engines.

Burst testing of a gelcast spin test rotor having a cast diameter over 8" has demonstrated over 2.5 times the engine design stress. A rotor disk having twice the cast diameter, as well as a thicker hub has also been gelcast successfully.

A radial turbine wheel applicable to microturbines and having improved FOD resistance has been designed with manufacturing ease as a primary criterion.

Technical Progress

Task 1 - Simulation of Production Environment

AS800 continues to demonstrate the high, lot-to-lot consistency of mechanical properties required for heat engine applications. (Note: A lot represents a single, mill-batch of AS800.) Combining 280 flexural specimens covering 14 slipcast lots in a maximum likelihood (mle) Weibull analysis resulted in a characteristic strength of 760 MPa with a Weibull parameter of 16 at room temperature. Gelcast AS800 (16 lots, 320 flexural specimens) exhibited a characteristic strength of 730 MPa with a Weibull parameter of 16. This analysis applies to uncensored flaw populations, although in almost all cases fracture initiated at large grains. The slightly lower strength of gelcast AS800 is due to the fact that the longer sintering cycle required to densify a material with lower green density results in a slightly larger grain size. At 1370°C, the Weibull parameter for 20 slipcast lots was 19 (190 specimens) and for 16 gelcast lots (160 specimens) it was 16. Fracture toughness was determined on two flexural bars from each lot by the indent retained strength method. The measured values were 8.2 and 8.1 $MPa \bullet m^{1/2}$ for slipcast and gelcast AS800 respectively. These values were also very consistent, having

Weibull slopes of 20-40. It is important to note that a variety of raw material lots were used in processing the multiple lots tested, so the data are representative of production conditions.

Tensile strength data determined on buttonhead test specimens are given in Table 1.

Table 1: Room Temperature Tensile Strength of AS800

	Characteristic Strength (MPa)	Weibull	Number of Specimens/Lots
SLIPCAST AS800	740	32	79/16
GELCAST AS800	653	14	76/16

For slipcast AS800, the tensile data were even more consistent than the flexural data. The high Weibull modulus of 32 was determined by testing 79 specimens representing 16 material lots, and is particularly impressive. The characteristic strength and Weibull modulus for gelcast AS800 were somewhat less. Fractography of the tensile specimens indicated that the lower strength and higher variability were due to failures at pores, inclusions, and clusters of large grains, defects that were not observed in the flexural tests due to the small volume being sampled. Processing refinements are being evaluated to eliminate these types of flaws.

Although the data are not as extensive, the 1200°C tensile stress rupture data for slipcast

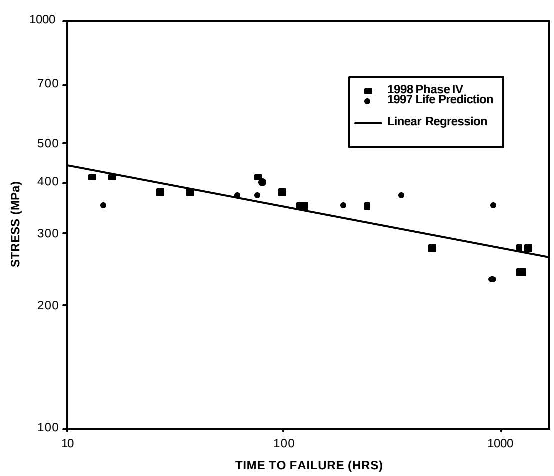

AS800 were also consistent. Five specimens from three lots of material were tested, and as shown in Figure 1, the data are identical to previous data obtained under the Life Prediction Program conducted by AlliedSignal Engines, also funded by the Department of Energy.

Task 2 - Fabrication Process Characterization

Task 1 is demonstrating that the up-front, powder processing (batching, milling, casting etc.) for production slipcast AS800 is under control. Gelcast AS800 is a relatively immature material and has room for improvement. Task 2 offers the opportunity to achieve improvements in the strength and consistency of gelcast AS800 through a better understanding of the fabrication process. However, gains are often difficult to measure since many specimens on multiple lots are required to achieve the level of confidence that justifies a process change. Nonetheless, several process changes have been evaluated.

Silicon nitride cannot be sintered without the addition of liquid forming sintering aids. To achieve the desired slurry characteristics, these are added to gelcast mills later in the milling cycle than they are in slipcast mills. Since inadequate mixing of the sintering aids could result in the large grain clusters observed in the fractography of gelcast tensile bars, a change in the timing was evaluated. Very early additions increased the viscosity of the slurry and were unacceptable. Later additions did not cause a processing problem, and plates for buttonhead tensile specimens were cast and machined. Although no large grain clusters were observed, three of five specimens tested at room temperature did not fail at large grains as desired. This may indicate that the timing of the addition is important but further studies are required to justify a change in the current production practice.

A second experiment designed to address the observation of inclusions involved filtering gelcast slurry at two levels. A limited number of buttonhead tensile tests were performed (five for each filtering level), and nine of ten specimens failed at large grains as desired. However, one specimen failed at a porous region that was cause for concern since filtering the viscous gelcast slurry could cause cavitation and entrain air. Flexural specimens all failed from large grains, but this is typical of flexural tests. Since the Weibull of 14 was lower than expected, there was no obvious benefit of slurry filtering.

In a third experiment performed under Task 2, the benefit of an oxidation heat treatment for machined surfaces of AS800 was evaluated. In this study, both longitudinally machined and transverse-machined, flexural test bars were heat treated in air at three different temperatures for three different times. The slipcast data are given in Table 2. It is evident that all of the treatments are capable of healing the machining damage observed for transverse-machined surfaces. In fact, the heat treatment actually increases the strength except at the highest temperatures and longest times, where a significant oxide layer is being formed.

Table 2. Oxidation Heat Treat Results for Slipcast AS800

Condition	15 Longitudinally Machined Test Bars	5 Transverse Machined Bars
	Strength (MPa)	Strength (MPa)
Baseline	739 ± 46	651 ± 11
T_1/t_1	794 ± 50	835 ± 14
T_1/t_2	794 ± 48	820 ± 28
T_1/t_3	831 ± 61	823 ± 49
T_2/t_1	791 ± 43	780 ± 30
T_2/t_2	819 ± 45	824 ± 41
T_2/t_3	805 ± 46	789 ± 25
T_3/t_1	807 ± 43	790 ± 39
T_3/t_2	750 ± 64	745 ± 77
T_3/t_3	730 ± 62	753 ± 39

Corresponding results for gelcast AS800 are shown in Table 3. As expected, the baseline strengths are similar and the treatments heal the transverse machining damage. However, the heat treatments do not increase the gelcast strength above the baseline. This difference in behavior between slipcast and gelcast is not yet understood. However, it would appear to be beneficial to give most machined parts a mild oxidation heat treatment to eliminate machining damage, as there are typically areas on engine components with machined surfaces where the principle stress is transverse to the direction of the machining grooves.

Table 3. Oxidation Heat Treat Results for Gelcast AS800

Condition	15 Longitudinally Machined Test Bars	5 Transverse Machined Bars
	Strength (MPa)	Strength (MPa)
Baseline	734 ± 62	629 ± 17
T_1/t_1	710 ± 42	719 ± 43
T_1/t_2	731 ± 22	723 ± 13
T_1/t_3	733 ± 36	751 ± 30
T_2/t_1	711 ± 48	707 ± 51
T_2/t_2	724 ± 46	742 ± 47
T_2/t_3	704 ± 65	725 ± 28
T_3/t_1	701 ± 36	725 ± 41
T_3/t_2	685 ± 49	692 ± 39
T_3/t_3	676 ± 56	582 ± 19

The final effort under Task 2 was in the area of densification. Since a longer sintering cycle is required to densify gelcast AS800 due to its lower green density, it received priority. A design of experiments (DOE) approach was used. Factors included top temperature, intermediate temperature, gas pressure profile, and crystallization conditions. Although all of these variables were found to influence the microstructure and density, the gas pressure at various stages in the sintering cycle had the greatest effect. This initial DOE has been followed up with more focused experiments, and a tentative new cycle has been established. The implementation of this cycle awaits sufficient data over a period of time to justify the change.

Task 3 - AS800 Oxidation Improvement

The focus of the oxidation improvement task has changed since the inception of the program. Initially, the goal was to explore compositional modifications of AS800 to reduce the rate of cyclic oxidation. However, NASA researchers published results on the volatility of silicon oxide in combustion gases with high water vapor content, an atmosphere representative of typical gas turbine engine combustor. Both silicon nitride and silicon carbide depend on the silicon oxide layer to protect them in oxidative environments, and as the layer vaporizes, both material recession and continued oxidation occur. Testing of AS800 turbine nozzles for 800 h in an industrial, gas turbine engine operating at peak temperature resulted in measureable dimensional changes due to material recession. As a result, the focus has changed to protective coatings, and a proprietary coating is currently being evaluated. This coating can be applied by conventional processes [e.g., electron beam – physical vapor deposition (EB-PVD) and plasma spray]. It is stable in combustion gas environments, and due to the thermal expansion match with AS800 and the preparation of the AS800 surface, it is adherent. Thermal cycling tests and oxidation tests in high, water-vapor environments are currently underway.

Task 4 - Gelcasting of Large, Thick Section Turbine Rotors

During the successful development of an integral slipcast AS800 axial turbine rotor for the 331-200 gas turbine engine, non-bladed spin test rotors were fabricated and tested to failure to demonstrate that the strength of the material in the rotor hub was consistent and met the requirements of this application. This same spin test rotor, approximately 8 in cast diameter and 2.25 in hub thickness, was selected for Task 4. Spin casting was also selected, since this is the same process that would be used to cast bladed rotors. A number of gelcast AS800 spin test rotors were fabricated and two parts were final machined - in the hub area for the attachment and on the O.D. for spin balance. These parts failed at 66,750 and 69,150 rpm, the high end of the burst test results previously obtained for slipcast spin disks. Typically, the burst test requirement for a rotor is set at 120% of design speed in the engine. Since the stress increases as the square of the speed, this is equivalent to 144% of design stress. The average burst test speed of 67,950 obtained for the gelcast rotor is equivalent to 265% of design stress, a large margin. Fractography of the burst fragments showed that both disks failed from single large grains as desired. Although only two disks were burst tested, the results are better than could be predicted by the tensile data obtained under Task 1, since the spin test rotor has considerably more volume under stress than a buttonhead tensile specimen.

Since the development of the gelcast 331-200 spin test rotor was so successful, a mold was designed and fabricated for a larger rotor disk, 16-in cast diameter, 3-in hub thickness, and weighing 15 kg after drying. Spin casting was also used for this part. The first disk stuck to the mold due to scrubbing of the mold release agent as the slurry, which was being poured into the center of the mold, was slung to the O.D. This was solved by partially static-filling the mold prior to spinning. Since the slurry assumes a parabolic shape during spinning, the amount required to maintain coverage of the mold bottom can be calculated. Another part cracked due to rapid cooling after gellation. Using forced-air cooling which was much slower solved this problem. The fourth disk was cast without problems and awaits densification. Although the 16-in-dia part fits in the furnace, there is concern that thermal stresses due to temperature gradients during heat-up will be sufficient to crack the disk. As a result, a slow heating procedure for the furnace is being

developed. Figure 2 shows both the 16in-dia, gelcast disk and the 8-in-dia gelcast 331-200 spin test disk. The slipcast integral rotor and slipcast inserted rotor blade are shown for comparison.

Task 5 – Ceramic Radial Turbine Wheel Design

The preliminary design of a gelcast, radial turbine wheel was completed during 1999. This rotor has thicker airfoils for improved FOD (foreign object damage), has been designed for manufacturability, and has been analyzed for acceptable structural life using the database developed under Task 1.

Status of Milestones
All milestones have been achieved.

Industry Interactions
AlliedSignal Ceramic Components has ongoing discussions with potential microturbine manufacturers and ATS (Advanced Turbine Systems) program participants to apprise them of material capabilities, assess their ceramic needs, and service customer requirements.

Problems Encountered
None.

Publications
None.

Characterization of Monolithic Silicon Nitrides for Microturbine Applications

G. A. Graves, S. Goodrich, D. Grant, J. S. Hilton, N. Osborne, and M. Pierson, University of Dayton Research Indstitute

Objective

The objective of this project is to work closely with materials suppliers to characterize monolithic ceramics and provide the data obtained to microturbine manufacturers via web-site data. The types of tests performed in the characterization studies can include flexural strength (4-point-bend and ring-on-ring), tensile strength, slow crack growth (dynamic fatigue), compressive strength, creep/stress rupture, oxidation determinations, Young's modulus and Poisson's ratio, coefficient of thermal expansion (CTE), fracture toughness, microhardness, microstructural studies, and fracture analysis.

Highlights

During the reporting period, the latest vintage of AlliedSignal AS-800 silicon nitride (Si_3N_4) material, both slipcast and gelcast, was tested at room temperature in tension. The slipcast material produced a Weibull modulus that is believed to be the highest ever recorded for a monolithic (Si_3N_4) ceramic at room temperature (21°C). In addition, the characterization of Kyocera SN-281 and SN-282 Si_3N_4 materials continued. Flexural strength and dynamic fatigue determinations are being determined at 21 and 1260°C on as-sintered, sintered and heat-treated, and machined and heat-treated material.

Technical Progress

Monolithic Ceramics In July 1999, a batch of 25 AS-800 Si_3N_4 slipcast and 25 gelcast buttonhead tensile specimens (standard buttonhead configuration) were received from AlliedSignal Ceramic Components, Torrance, CA. The two batches of AS-800 were tested in tension, at room temperature (21°C) at a stress rate of 150 MPa/s. The gelcast material had an average tensile strength of 642 MPa (93.2 ksi) with a standard deviation of 52.4 MPa (7.6 ksi). The slipcast material had an average tensile strength of 726 MPa (105 ksi) with a standard deviation of 21 MPa (3.0 ksi).

The Weibull plots for both the gelcast and slipcast specimens are shown in Figure 1. The Weibull parameters (m) of nearly 38 for the slipcast material are extremely high for a monolithic ceramic. In early vintage AS-800 material, large voids (Figure 2) and large agglomerated grains (Figure 3) were evident at fracture initiation sites. In the latest vintage slipcast material, only isolated large grains (Figure 4) were found at fracture initiation sites. This may be the reason for the high strength and low data scatter.

Groups of ten Kyocera SN-282 sintered and heat-treated specimens were tested in flexure at 1260°C at stressing rates of 0.1, 1, 10, and 500 MPa/s to determine slow crack growth parameters. One group of ten specimens was also tested at room temperature (21°C). Ultimately similar tests will be performed on as-received sintered, sintered and heat-treated, and machined

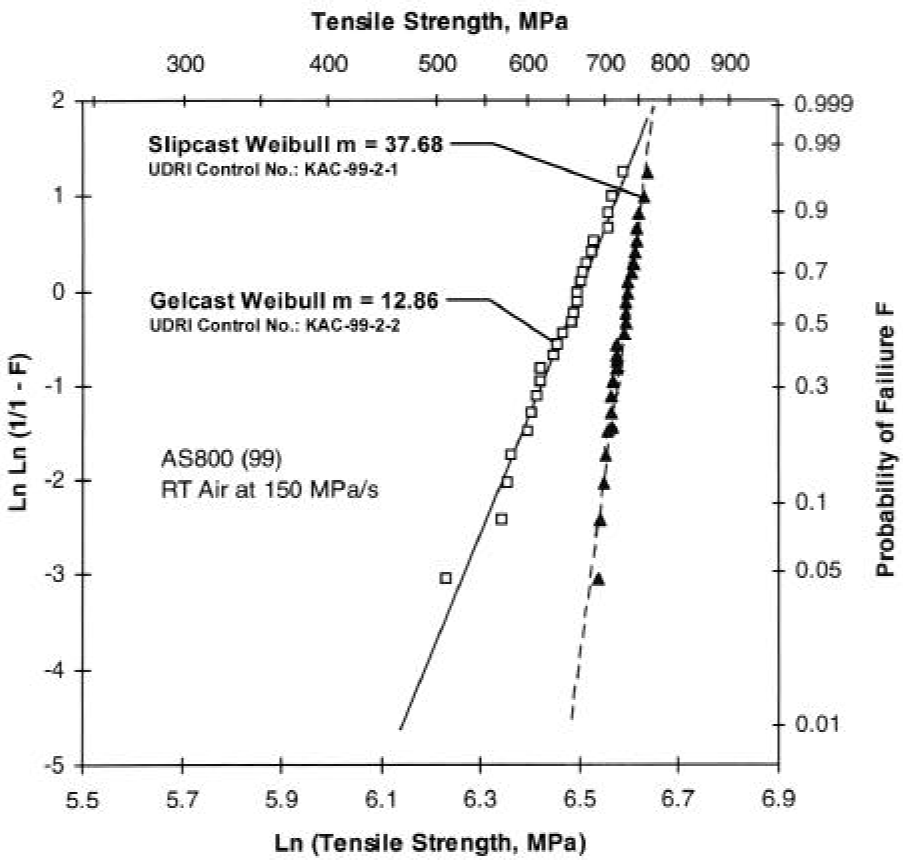

Figure 1. Weibull plots of the latest vintage (1999) AlliedSignal Si_3N_4 AS-800 (gelcast and slipcast).

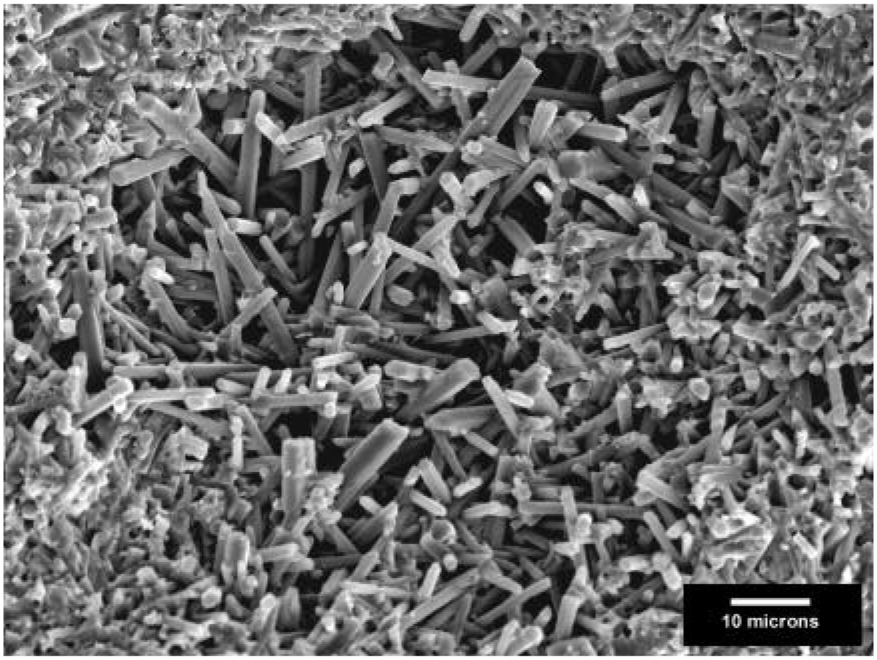

(i990474.tif)

Figure 2. SEM photomicrograph of large voids found in earlier vintage (1998) AlliedSignal AS-800 Si_3N_4 at fracture initiation sites.

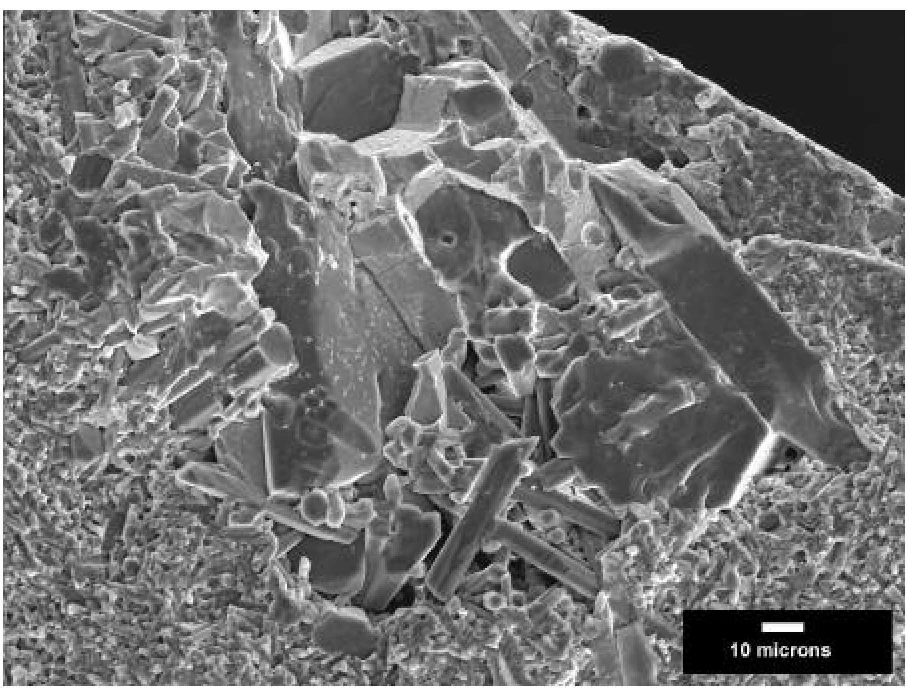

(i981780.tif)

Figure3. SEM photomicrograph of large agglomerated grains found in earlier vintage (1998) AlliedSignal AS-800 Si_3N_4 at fracture initiation sites.

(i991116.tif)

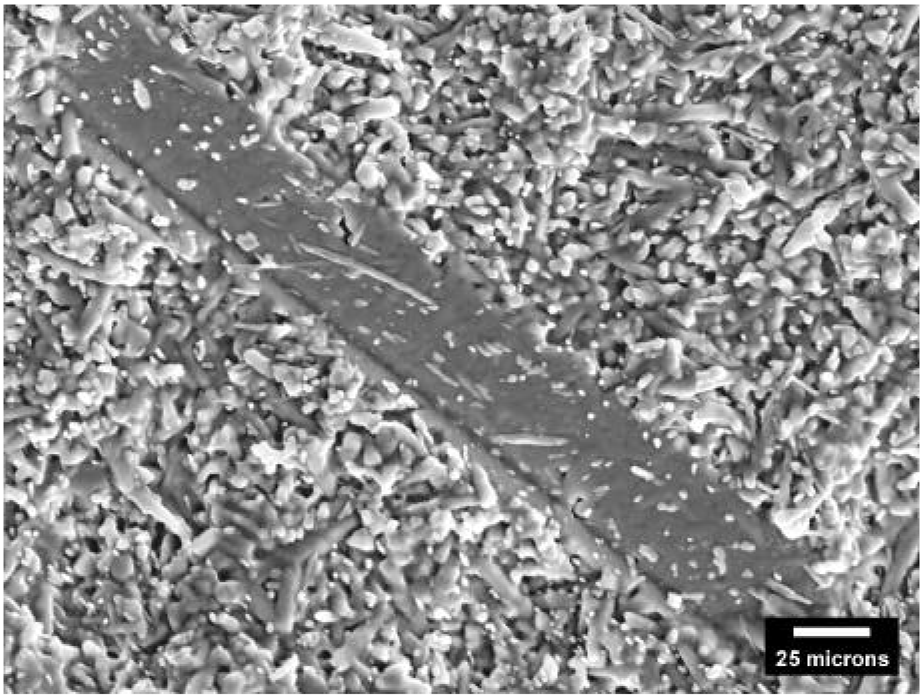

Figure 4. SEM photomicrograph of single large grains found in the latest vintage (1999) AlliedSignal AS-800 Si_3N_4 at fracture initiation sites.

and heat-treated SN-281 and 282 specimens. Slow crack growth and Weibull parameters will be determined for each group of material and microstructural and fracture analysis will be performed.

Five SN-281 tensile creep/stress rupture tests were initiated late in the reporting period. The results will be reported in the next quarterly report.

The project to put additional DOE, Oak Ridge, and UDRI structural ceramic data on the UDRI web site (http://www.udri.udayton.edu/handbook/title.html) has also continued.

Status of Milestones
Monolithic Ceramic Characterization: on schedule
Web Site Ceramic Data Base: on schedule
Creep/Stress Rupture Testing: on schedule

Industry Interactions
Numerous telephone conversations with Dr. James Wimmer, AlliedSignal Ceramic Components.

Problems Encountered
None.

Publications
None.

COMPONENT VERIFICATION

H. T. Lin, M. K. Ferber, and P. F. Becher, Oak Ridge National Laboratory

Objective

Evaluate and document the long-term mechanical properties of very small specimens machined from complex-shaped ceramic components (e.g., blades, nozzles, vanes, and rotors) at elevated temperatures under various controlled environments. This work will allow end users to verify mechanical properties of components and apply the component database generated for advanced design and lifetime prediction analyses. Generate mechanical properties database for ceramic recuperator materials. The database will be used for the finite element analysis of life prediction of the recuperator components employed in microturbine systems.

Highlights

Biaxial mechanical tests on disk samples extracted from AlliedSignal Ceramic Components (ASCC) AS800 silicon nitride, first-stage vanes have been completed. The vanes are designed and fabricated for the Rolls-Royce Allison Model 501-K turbine engines and have been successfully field tested for up to 815 h at the Exxon natural gas processing plant in Mobil, AL. The operating conditions of Allison Model 501-K engine are approximately 1010°C, 6-8% water vapor, and 130-psi gas pressure. Disk-shaped samples (6-mm dia and 0.5-mm thickness) were extracted from platform and airfoil sections from as-processed vanes and from vanes exposed for field-test times ranging from 22 to 815 h. Note that specimens were tested such that the exposed external surfaces were the tensile surfaces. Results indicate that the fracture strengths exhibit increased scatter after ~ 200 h into the filed tests. However, the average strength remains relatively constant. The strengths of the specimens extracted from the airfoil surfaces tend to be slightly lower than those from the platform sections and from as-processed vanes. The slight decrease in fracture strength of samples from airfoil sections is attributed to the relative deep environmentally-affected zone (EAZ, ~ 50 μm) as compared to those from platform sections and as-processed vanes (~ 15-20 μm).

Technical Progress

During this reporting period, research efforts focused on the evaluation of ceramic materials fabricated by Kyocera and ASCC for the Solar Turbines CSGT program. Mechanical testing and microstructural analyses were carried out on AS800 silicon nitride, first-stage turbine blades fabricated by ASCC and SN88 silicon nitride, first-stage nozzles fabricated by NGK as shown in Figure 1. Both AS800 turbine blades and SN88 nozzles, designed for the Solar Centaur 50S turbine engine, have been successfully field-tested for 1050 h and 68 h, respectively. The operating conditions of the Solar Centaur 50S engine are approximately 1010°C, 15% water vapor, and 150 psi gas pressure. Disk-shaped specimens (6-mm dia and 0.5-mm thickness) and bend bars (2 x 3 x 30 mm) were extracted from both airfoil and platform sections for mechanical property evaluation at room temperature. The data for the field-tested components were compared with that obtained from the production billets and as-processed components to evaluate the effect on mechanical properties of long-term exposure to a combustion environment. Subsequent detailed microstructural and X-ray analyses were also carried out to investigate the effect of combustion exposure on the stability of microstructure and chemistry of secondary phase(s). Results of microstructural analyses and mechanical property evaluation provide very important feedback on the reliability and survivability of specific silicon nitride engine components. In addition, the strength results for the specimens from airfoil sections provide, for the first time, data needed for component design and lifetime prediction.

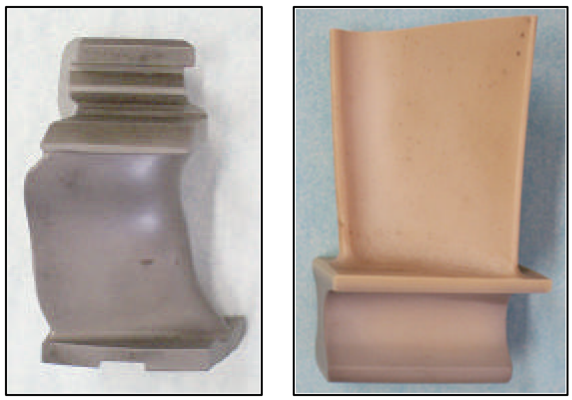

SN88 Nozzle AS800 Blade

Figure 1. Silicon nitride ceramic components employed in Solar Turbines Centaur 50S engine.

Tensile creep tests on small, dog-bone, tensile specimens extracted from NGK SN88 silicon nitride gas turbine nozzle (Fig. 2) were also initiated during this reporting period. Tensile creep tests were carried out at 1350°C in air due to the availability and extensive creep properties database that were generated by various laboratories with large production billets using various specimen sizes and configurations. Preliminary results indicated that the specimens extracted from production ceramic nozzles exhibited creep rates that were ten times higher than those obtained from the billet shapes as shown in Figure 3. Similar differences in creep rate between ceramic components and production billets have been reported for NT164 turbine blades [1].

Tensile creep specimens of Kyocera SN281 and SN282 silicon nitride materials have also been prepared during this reporting period. Both the SN281 and SN282 silicon nitride materials are candidate materials for applications as gas turbine components (e.g., blades, nozzles, and vanes). Creep tests at temperatures ranging from 1316 to 1400°C in air will be initiated to generate a creep property database for life prediction.

Exposure of various, commercially available silicon nitride ceramics to high-temperature, water-vapor environment has also been initiated during this reporting period. The objective of this study is to provide an insight into the effect of long-term exposure to a simulated combustion environment on the stability of microstructure and chemistry, and thus, mechanical reliability of silicon nitride materials. All exposure tests were

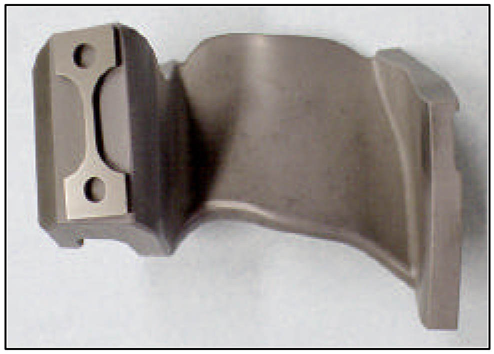

Figure 2. Small dog bone type tensile creep specimen extracted from Solar SN88 silicon nitride first stage nozzle.

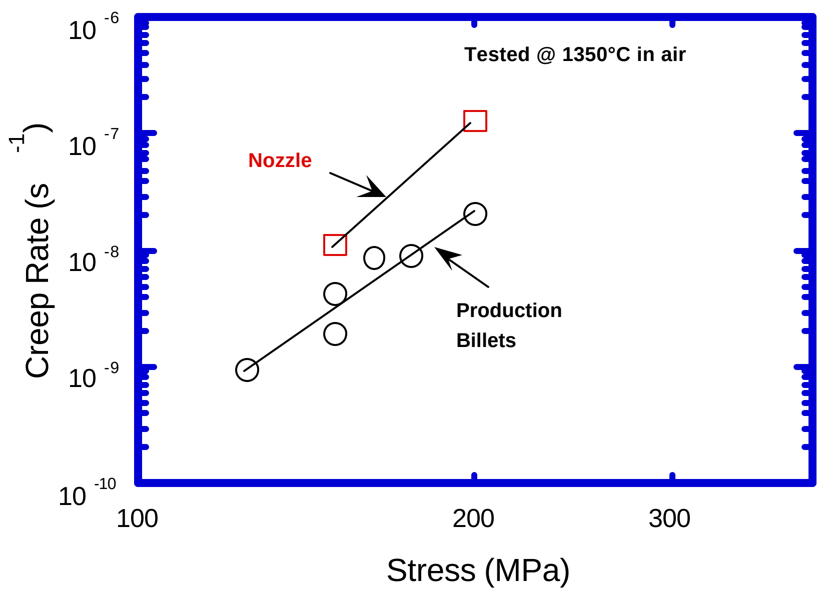

Figure 3. Creep rate versus applied stress curves at 1350°C in air for specimens extracted from NGK SN88 ceramic nozzle.

conducted at 150 psi, 1204°C, 15% steam in exposure increments of 500 h. Microstructural evaluation was carried out after each 500 h exposure to characterize the extent of surface damage and to determine degradation mechanisms for different silicon nitride ceramics. Mechanical properties (i.e., strength and creep resistance) of some of the exposed samples were measured to determine the effect of combustion environment on the mechanical reliability and lifetime at elevated temperatures. Preliminary results indicated that the extent of surface oxidation and degradation of mechanical performance after long-term exposure to a high-temperature steam environment is strongly dependent upon the chemistry and microstructure of secondary phase(s) in silicon nitride ceramics.

Status of Milestones
On schedule.

Industry Interactions
Measured the mechanical properties of complex-shaped, ASCC AS800 silicon nitride, first-stage turbine blades; Kyocera SN281 silicon nitride, first-stage turbine blades; and NGK SN88 silicon nitride, first-stage nozzles and gave the data to all the ceramic component suppliers, as well as Solar Turbines.

Characterized the mechanical properties of ASCC AS800 silicon nitride, first-stage vanes after engine field tests and gave the data to ASCC and Rolls-Royce Allison Engines.

Jim Wimmer, ASCC, provided tensile creep specimens machined from slipcast AS800, simulated, airfoil plates for evaluation of component properties.

Dave Carruthers, Kyocera, provided SN281 and SN282 silicon nitride ceramic billets for generation of tensile creep database and study of long-term exposure to a simulated turbine engine environment.

Joe Aihara and Tsutomu Yamamoto, NGK Insulators, Nagoya, Japan, provided SN88 and SN84 silicon nitride ceramic materials for generation of tensile creep database and study of long-term exposure to a simulated turbine engine environment.

Roger Matsumoto and Phill Craig, ASCC, provided ceramic recuperator materials for mechanical property evaluation.

Problems Encountered
None.

Publications
1. H. T. Lin, P. F. Becher, M. K. Ferber, and V. Parthasarathy, "Verification of Creep Performance of a Ceramic Gas Turbine Blade," *Key Engineering Materials,* Vols. 161-163, 1999, pp. 671-674.
2. H. T. Lin, S. B. Waters, and K. Breder, "High-Temperature Creep Response of a Commercial Grade Siliconized Silicon Carbide," *J. Mater. Sci.* (in press).
3. M. K. Ferber, H. T. Lin, V. Parthasarathy, and W. Brentnall, "Degradation of Silicon Nitrides in High Pressure, Moisture Rich Environments," to be published in the Transactions of ASME, 1999 (ASME TURBO EXPO '99, June 7-10, 1999, Indianapolis, Indiana).

References

1. H. T. Lin, P. F. Becher, M. K. Ferber, and V. Parthasarathy, "Verification of Creep Performance of a Ceramic Gas Turbine Blade," *Key Engineering Materials,* Vols. 161-163, 1999, pp. 671-674.

Oxidation-Resistant Coatings on Silicon Nitride for Microturbine Applications

S. M. Zemskova, J. A. Haynes, K. M. Cooley, D. P. Stinton

OBJECTIVE

Silicon-based ceramics, such as Si_3N_4, are candidate structural materials for high-temperature components in small, land-based, gas turbine engines (microturbines). However, reaction with water vapor results in very rapid oxidation of silica-forming materials in elevated-pressure, high-gas-velocity combustion environments. Therefore, coatings that are capable of providing oxidation protection in the presence of water vapor will be necessary to ensure the long-term durability of Si_3N_4 components in microturbine combustion environments. It has been recently demonstrated that thin, dense coatings of chemical vapor deposition (CVD) mullite ($3Al_2O_3 \times 2SiO_2$) can provide excellent oxidation protection for Si_3N_4 and SiC in low-velocity, high-pressure steam. However, the microstructure and composition of CVD mullite are variable, depending on deposition conditions and substrate composition, and can substantially influence coating properties such as oxidation resistance, substrate interactions, and mechanical integrity. The influence of an oxide surface coating on monolithic ceramics mechanical properties is also of interest. The objectives of this project are to determine optimum coating microstructure, thickness, and composition (Al/Si ratio) for oxidation protection (based on results of testing in simulated combustion environments) and thermo-mechanical stability on Si_3N_4. Coating influence on the chemical and mechanical integrity of various Si_3N_4 materials will also be determined.

HIGHLIGHTS

Based on the results of numerous deposition parameter and characterization studies, deposition conditions for fabrication of thin, dense, uniform coatings of crystalline CVD mullite on Si_3N_4 bend bars were developed this quarter. However, there appears to be a coating thickness limit, after which coating growth instabilities occur, that could be related to the current reactor flow configuration. This issue is currently being addressed by reactor modifications (increase of gas velocities), so that thicker coatings can be deposited in upcoming quarters. Bend bars of various Si_3N_4 compositions have been thinly coated with CVD mullite. The as-coated specimens are currently being tested by four-point flexure at room temperature in order to determine whether the coating process or the presence of the thin surface coating significantly alters Si_3N_4 mechanical properties or failure modes. Coatings on Si_3N_4 were tested in a high-pressure steam rig (1200^{o}C, 10 atm pressure, 15% H_2O in air) in order to evaluate their protective capacity.

TECHNICAL PROGRESS

Optimization of Coating Deposition Parameters

The focus of work thus far has been aimed at the development of CVD parameters for fabrication (on Si_3N_4 bend bars) of dense, uniform, crystalline mullite coatings with controlled Al:Si ratios. Successful deposition of mullite coatings was previously demonstrated over the temperature range 950-1050°C, but microstructural control was difficult, especially at the higher temperatures. Thus, optimization of other CVD parameters (total pressure, gas ratios and gas flow rates) was necessary in order to obtain better control of coating microstructure and Al/Si ratio.

The horizontal, hot-wall reactor used for fabrication of CVD mullite coatings consisted of an alumina tube, with an inside diameter (ID) of 5.0 cm and a length of 48.0 cm, sealed at both ends by a pair of stainless steel flanges with compression O-ring fittings. An annular, cylindrical, graphite susceptor sealed in fused silica (ID = 5.7 cm, OD = 7.4 cm, and length = 15.2 cm) was placed around the reactor tube and heated by a 20kW radio-frequency generator. The effective heating zone was 18.0 cm in axial length, with a uniform temperature zone of approximately 5 cm in length at the center (the general temperature profile across the hot zone was parabolic in nature, with a maximum at the center). Temperature was maintained by a K-type thermocouple and a controller and varied within the uniform zone by ±10°C. The reactor gas lines were constructed of electro-polished stainless steel tubes, and connectors were made with metal gasket fittings in order to minimize leaks. Reactor pressure was controlled by a throttling valve interfaced with the pressure controller and a capacitance manometer.

Mullite coatings were fabricated via CVD by the reaction:

$$6AlCl_3 + 2\ SiCl_4 + 13CO_2 + 13H_2 = 3Al_2O_3 \times 2SiO_2 + 13CO + 26HCl$$

Aluminium trichloride was formed in situ by flowing HCl through a vaporizer at 200°C to react with Al pellets (i.e., $Al + 3HCl = AlCl_3 + 1.5H_2$). Silicon tetrachloride vapor was introduced from liquid source via an Ar carrier gas. The $SiCl_4$ bubbler was immersed in a refrigerated bath at a temperature of -20°C. CO_2, H_2, and Ar were mixed with the chlorides prior to entering the reactor. Mass flow controllers were used to control the gas flow rates.

Earlier, the effects of deposition time, specimen position within the reactor hot zone, and $SiCl_4$ vapor pressure on mullite coating microstructures were studied [1,2]. Here, all coatings were deposited at a reactor pressure of 80 torr for two h. Experiment variables were deposition temperatures, gas flow rates, and specimen position (i.e., location within the hot zone) (Table 1).

Table 1. Ranges of CVD Mullite Deposition Parameters Investigated in Optimization Study

Deposition Temp (°C)	950, 1000, 1050	**Ar flow rates**	400, 250, 190, 150
System Pressure	80 torr	**H_2 flow rates**	1000, 600, 300
$SiCl_4$ Temp (°C)	-20	**CO_2 flow rates**	100, 50
HCl flow rate	20	**$SiCl_4$ flow rates**	10.0, 8.5, 7.0, 5.0

The effects of reactor position are a concern due to the potential influence of down-stream reactant depletion on coating microstructure and composition. As-machined Si_3N_4 coupons (1.0×1.0×0.3 cm) were placed on an alumina fixture divided into five equal parts identified as position N1 (upstream, nearest injector), N2, N3, N4, and N5.

Two coupons (positions N2, N4) or three coupons (positions N1, N3, N5) were coated during the same experiment. After coating optimization, two side-by-side Si_3N_4 bend bars (0.4 x 0.3 x 5.0cm) were coated during each experiment (centered).

Phase identification was accomplished via X-ray diffraction (XRD) (PAD V, Scintag, Sunnyvale, CA). The microstructures and compositions of coating surfaces and metallographic cross-sections were evaluated by field-emission gun, scanning electron microscopy (FEG-SEM) (S-800, Hitachi, Tokyo, Japan) and energy dispersive X-ray spectroscopy (EDS). Typical results are summarized in Table 2.

Table 2. Characterization of CVD Mullite Coatings

Sample ID	**Tem., °C**	**H_2 flow**	**CO_2 flow**	**$SiCl_4$ flow**	**Ar flow**	**Weight gain, mg**	**Phase (XRD)**	**Al:Si ratio (EDS)**
M040699 1,3,5	950	300	50	10	190	0.2/0.2/0.2	mullite	3.9/2.8/1.1* *1.2***
M060299 1,3,5	950	600	100	10	400	1.2/1.2/1.0	mullite	6.6/5.9/4.3 *4.4*
M070999 1,3,5	1000	300	50	10	150	1.2/1.2/0.9	mullite	3.0/3.1/3.0 *2.5*
M070899 1,3,5	1050	300	50	10	150	3.2/2.7/2.7	mullite	4.4/4.6/4.8 *4.0*
M060999 1,3,5	1050	600	100	10	400	4.1/4.8/4.2	mullite	8.9/4.8/4.5 *5.5*
M051499 1,3,5	1050	1000	100	10	250	5.7/2.6/8.1	mullite	very low Si content
M080699 2,4	1000	300	50	5	150	2.2/2.1	mullite	very low Si content
M080599 2,4	1000	300	50	7	150	2.6/2.3	mullite	2.9/3.2 -
M081999 1,3,5	1000	300	50	8.5	150	1.6/1.8/2.2	mullite	4.3/4.1/4.6 -
M081399 2,4	1000	300	50	8.5	150	1.5/1.3	mullite	3.8/3.2 *3.8/3.1*

*surface scan; **cross-sections scan

Effect of Deposition Temperatures on Coatings Composition and Microstructure

The coatings M0406991,3,5; M0709991,3,5; and M0708991,3,5 were deposited under identical gas flow conditions and different temperatures: 950, 1000, and 1050°C. Specimen weight gain and coating thickness increased (from ≤1μm to ~2μm) as temperature increased (2 h standard deposition time). The morphology of the coatings deposited at 950°C can be described as an agglomeration of very fine, shapeless particles (Fig. 1a). Coatings deposited at 1000°C were relatively smooth, while large agglomerates of faceted cubic particles were observed at the surfaces of coatings deposited at 1050°C. The images of the coating cross-sections (Fig.2) show that coatings deposited at 1000°C were uniform in thickness.

Al:Si ratios of the coatings deposited at 950°C varied substantially with the positions of the specimens, from 3.9 (position N1) to 1.1 (position N5), while coatings deposited at

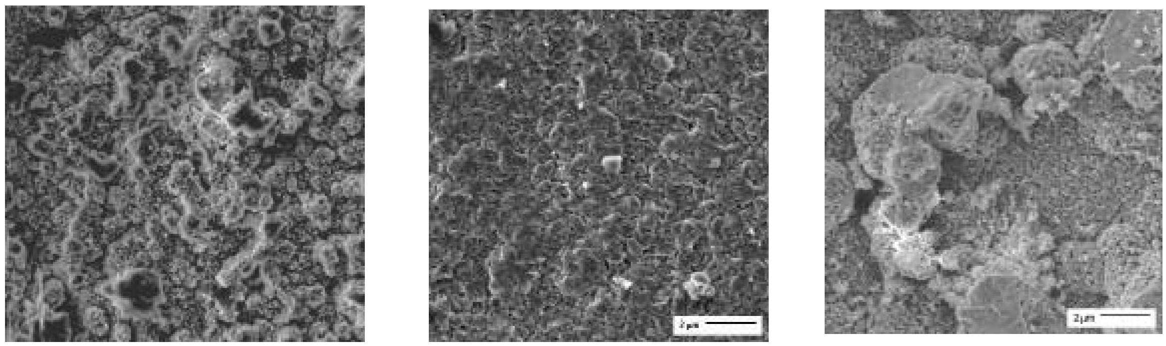

Fig. 1. SEM images (5K magnification) of the coatings surfaces deposited at 950 (a), 1000 (b) and 1050°C (c).

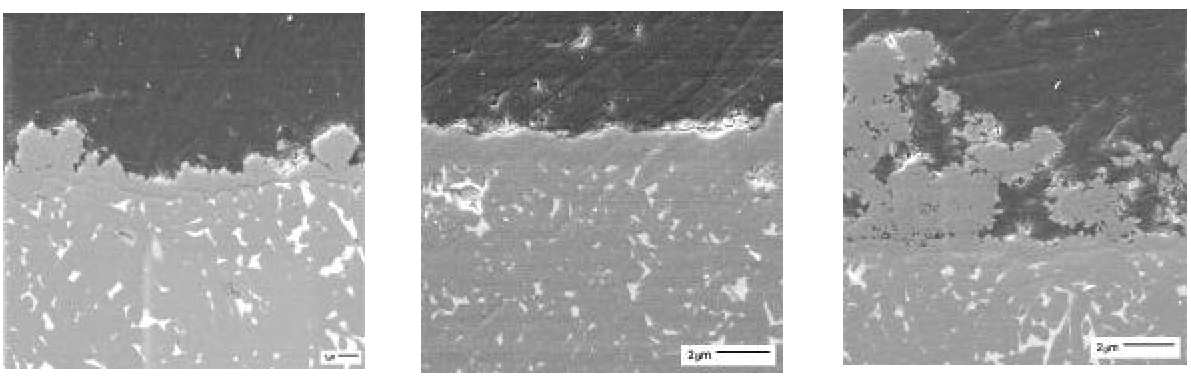

Fig. 2. SEM images (5K magnification) of the coatings cross-section; deposition temperatures were 950 (a), 1000 (b) and 1050°C (c).

1000 and 1050°C exhibit uniform chemical compositions for all three specimen positions (N1, N3, N5). The average Al:Si ratios increased from 2.6 to 3.0 to 4.6 with increasing deposition temperature.

Effect of Ar/H_2/CO_2 Flow Rates on Coatings Composition and Microstructure

In another set of experiments (M060291,3,5; M0609991,3,5; M0514991,3,5), gas flow rates were increased as follows: H_2-600/1000, CO_2-100, Ar-250/400. When hydrogen flow rate reached 1000, EDS spectra of the coatings showed very low silicon contents (Al:Si ratios ≥10) although XRD analysis still indicated the presence of the mullite phase.

The surfaces of coatings deposited at 950°C at higher gas flow rates was quite smooth and consisted of cubic crystalline particles. The same type of particles were observed at the surface of coatings deposited at 1050°C, but they were hemisphericaly-shaped and agglomerated. Some powder formation occured under these deposition conditions (Fig. 3a,b). Hence, the cross-sections show that dense and uniform coatings of ~1.5 μm thickness were deposited at the lower temperature (Fig.3c). The coatings deposited at 1050°C can be described as consisting of two layers: a thin (less than 1μm), dense layer is formed initially. At some point, coating growth becomes less stable and large agglomerates grow on top of the initial layer resulting in a high level of near-surface porosity and surface roughness (Fig.3d).

Al:Si ratios of the coatings deposited at high gas-flow rates increased substantially indicating the formation of an "alumina-rich," mullite phase. In addition, coating compositions varied substantially with specimen position (see Table 2.).

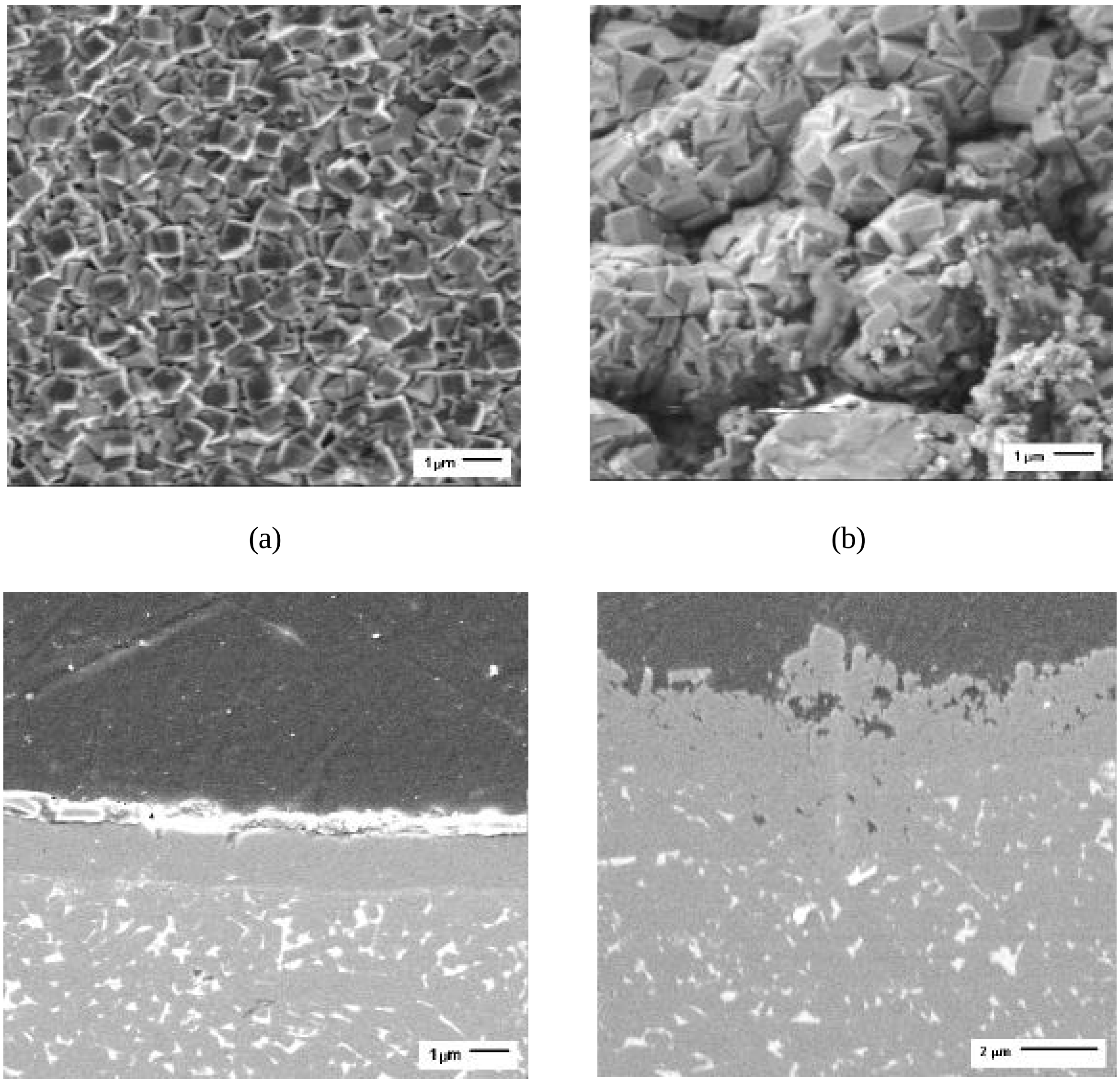

(a) (b)

(c) (d)

Fig.3. SEM images (5K magnification) of the surfaces and cross-sections of coatings deposited at higher gas flow rates of H_2-600, CO_2-100, Ar-400 and temperatures 950°C (a,c) and 1050°C (b,d).

Effect of $SiCl_4$ Flow Rate on Coating Composition and Microstructure

Based on the results described above, in order to study the effect of $SiCl_4$ flow rates on coatings compositions and microstructures, the CVD conditions were fixed as follows: deposition temperature - 1000°C, gas flow rates - H_2-300, CO_2-50, Ar-150. XRD analysis of the coatings deposited at the lowest $SiCl_4$ flow rate of 5 sccm (specimens M0806992,4) shows the formation of the mullite phase, but EDS spectroscopy indicates a very low silicon content (Al:Si ratios ≥10, surface scan). Coating surfaces consisted of very small particles, as well as large agglomerates (Fig.4a). Increasing the $SiCl_4$ flow rate to 7 sccm (samples M0805992,4) improved the particle crystallinity but caused further hemispherical agglomeration, as observed in the coatings deposited at high temperature and high gas flow rates (see Fig. 3b).

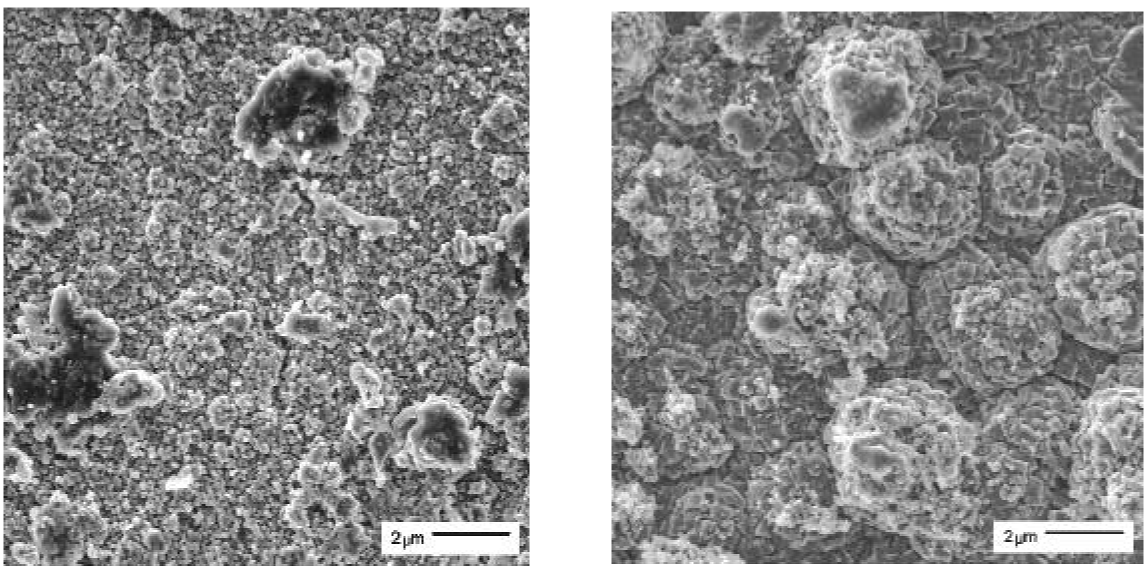

(a) (b)

Fig. 4. SEM images (5K magnification) of the coatings surfaces deposited at $SiCl_4$ flow rates of 5 (a) and 7 (b).

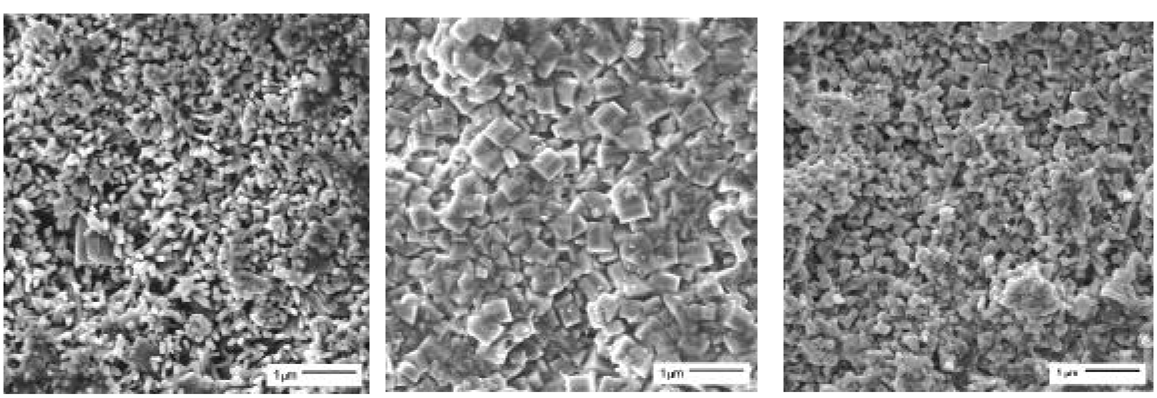

(a) – M0819991 (b) – M0819993 (c) – M0819995

Fig. 5. SEM images (10K magnification) of the coatings surfaces deposited at $SiCl_4$ flow rates of 8.5.

Some additional details of the surface morphology are shown in Fig. 5 at a magnification of 10K. Coating M0819993, deposited at the very center of the reactor hot zone (position N3), consisted of crystalline cubic particles of larger size in comparison to that of M0819995 (position N5). Coating M0819991, deposited at the upstream position (N1), consisted of grains with a columnar structure. Experiments were also performed to obtain coatings at the reactor hot zone positions N2 and N4. Surface morphology of the coatings M0813992, 4 (Fig.6) appear the same as that of coating M0819993, so it was

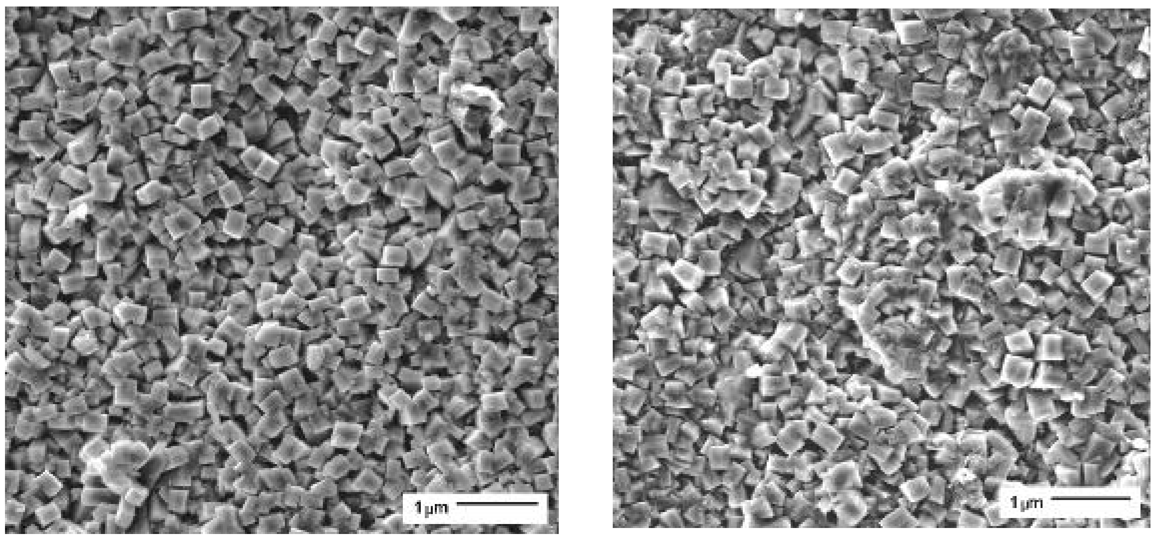

(a) M0813992 - position 2 (b) M0813994 – position 4

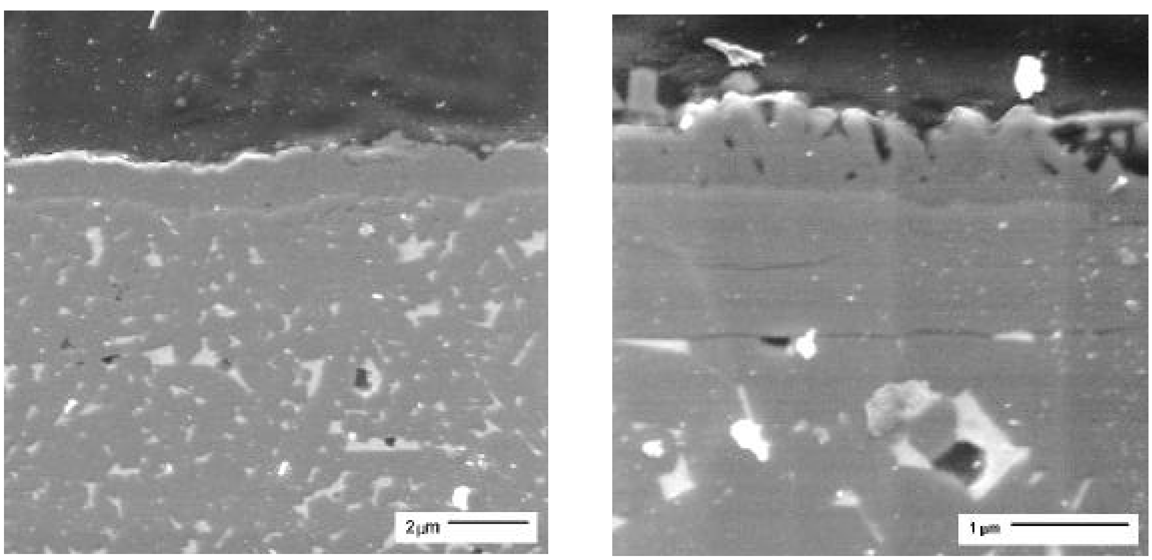

(c) M0813992, 5K (d) M0813994, 15K

Fig.6. SEM images of the surfaces (5K magnification) and cross-sections of the coatings deposited at $SiCl_4$ flow rates of 8.5.

concluded that under these deposition conditions, the center zone of ~3 cm (positions N1-N3) can be used to attain uniform, crystalline coatings on Si_3N_4 bend bars (which was a primary objective for this quarter). SEM images of cross-sections at 5K magnification show that the coatings appear dense and uniform in thickness (~2μm); some elements of a columnar structure can be observed at high magnification of 15K. Al:Si ratios of the coatings deposited at $SiCl_4$ flow rates of 7-8.5 varied from 2.9-4.6 indicating chemical compositions close to pure crystalline mullite phase (Al:Si=3.0). An important issue to be resolved is the capability of depositing thicker uniform coatings, since coating deposited for greater than 2 h displayed growth instabilities. Based on previous results, it is our hypothesis that increasing overall gas velocity through the reactor will improve this situation, thus, the inner diameter of the reactor is being reduced in order to accomplish this objective.

Fabrication of Mullite Coated Si_3N_4 Bend Bars for Mechanical Properties Testing

A systematic study examining the strength and fatigue resistance of mullite-coated, Si_3N_4 bend bars is being conducted. ASTM test procedures, using ASTM C 1161-B specimens, are being used to load specimen to failure in four-point flexure. Optical and SEM fractographic analysis of the fractured specimen surfaces will provide essential information regarding the variation of the mullite microstructure as it relates to mechanical behavior. An understanding of the failure mechanism(s) is essential for the successful implementation of mullite-coated Si_3N_4 in load -earing application.

Steam Rig Testing

High-pressure steam rig tests and steam thermal cycle tests are being performed on mullite-coated Si_3N_4 to investigate the protective properties and thermomechanical stability of CVD mullite coatings fabricated under optimized conditions. The effect of mullite Al:Si ratios on coatings oxidation resistance is being evaluated. The results obtained will provide a basis for formulation for scientific principles of design of advanced coating microstructures with optimum corrosion resistance.

Status of Milestones

We have achieved the milestone of optimizing CVD parameters for uniform coating of Si_3N_4 bend bars, as well as that of coating numerous bend bars for mechanical properties testing.

Industry Interactions

We have had discussion with both UTRC and AlliedSignal regarding coating of test components and testing of CVD mullite on Si_3N_4 in their burner rigs.

Problems Encountered

Under the current CVD reactor configuration, coating thickness limits were encountered, likely due to the low gas velocity in the relatively large volume of the reactor. This issue will be addressed by a slight reactor modification (insertion of a smaller diameter internal tube to increase gas velocity).

References

Haynes, J. A., Cooley, K. M., Stinton, D. P., Lowden, R. A., and Lee, W.Y., "Corrosion-resistant CVD Coatings for Si_3N_4," Ceramic Engineering and Science Proceedings (Cocoa Beach, Jan. 1999) in press.

Haynes, J. A., Lance, M. J., Cooley, K. M., Ferber, M. K., Lowden, R. A., and Stinton, D. P., "Protective Capacity of CVD Mullite Coatings in a High-Temperature, High-Pressure, Air-H_2O Environment," *J. Am. Ceram. Soc.*, (1999) in press.

Life Prediction Coordination

A. A. Wereszczak, Oak Ridge National Laboratory

Objective
Appropriate design and life prediction of ceramic components in microturbines will be critical to the achievement of 40% efficiency in these engines. There are four goals comprising this project: 1) collaborate with NASA and AlliedSignal Engines to help them further develop their respective probabilistic life prediction codes; 2) promote the use of structural ceramic life prediction codes to potential user, including the microturbine manufacturing community; 3) assist microturbine manufacturers with their use of the codes; and 4) interact with structural ceramic suppliers with the intent to promote material property optimization for microturbine ceramic components.

Highlights
The methodology used to predict the useful life of ceramic components in gas turbine engines has made great strides in the last five to ten years. There are, however, several areas that need additional development before ceramics can safely be used in advanced microturbines. The following statement summarizes those needs as identified by NASA and AlliedSignal Engines.

There is a need to enhance existing ceramic component life prediction computer programs so that they will incorporate environmental effects. Enhancements should include, but not be restricted to, the ability of these codes to perform meaningful ceramic component life prediction when the hot-section Si_3N_4 components are undergoing long-term degradation brought on by the turbines operating environment (i.e., high temperatures and pressures, moisture, oxidation), and/or are coated with an environmental barrier coating. Additional enhancements such as fatigue modeling for fully transient loadings, the consideration of engine-load histories, probabilistic creep analysis, and foreign and domestic object damage (FOD, DOD) modeling are also needed.

Technical Progress
Several communications with staff members at NASA (Noel Nemeth) and AlliedSignal Engines (Bjoern Schenk) occurred regarding the capabilities of current life prediction codes. Both codes being considered use probabilistic life design and can perform inert and fatigue life predictions as a function of temperature. Each code has some advantages and disadvantages compared to the other, but they have been shown to predict the same component response when the same inputs are used in the analysis. Capabilities of interest that both codes do not currently contain include: the consideration of environmental changes in silicon nitride components, and environmental barrier coatings of silicon nitride components.

Arrangements have been made to visit NREC during early Q1FY2000, and to discuss ceramic life prediction, recuperator, and silicon nitride issues with the staff at NREC in Portsmouth, NH. A presentation will be given that illustrates the structural ceramic life prediction algorithm using a ceramic diesel exhaust valve as the example component.

Several communications with AlliedSignal Ceramic Components' (ASCC) Jim Wimmer occurred regarding the high-temperature mechanical testing of AS800 on A. Wereszczak's Heavy Vehicle Propulsion Materials Program (DOE/OTT). There are some common denominators between the programs, and arrangements have been made for further discussion during a visit to ASCC in mid Q1FY2000.

Status of Milestones
No milestones due during present reporting period.

Industry Interactions
A number of interactions occurred with the following individuals during the present reporting period:

Advanced Ceramic Research	David Dent
AlliedSignal Ceramic Components	Jim Wimmer
AlliedSignal Engines	Bjoern Schenk
Kennametal	Russ Yeckley
Kyocera	Dave Carruthers
NASA	Noel Nemeth
NREC	Jim Kesseli
SUNY@Stony Brook	Alonso Peralta

Problems Encountered
None.

Publications
None.

NDE Technology Development for Microturbines

W. A. Ellingson and H. R. Lee, Argonne National Laboratory

Objective/Scope

The objective of the work in this project is to develop high-speed, production-rate, nondestructive evaluation (NDE) technology for gelcast microturbine rotors, also called "wheels." Gelcast production technology is under development to allow production volumes of 500-1000 rotors/mo. The work in this project has two parts: (a) development of NDE technology with a focus on higher yields to be realized through rejection of defective parts prior to binder removal and sintering, thereby utilizing furnace space for "good" parts, and (b) development of high-speed NDE metrology methods for verification of dimensions of as-cast wheels. This technology will impact mold design during process development to allow for variations in shrinkage in these complex designs, as well as verify final, as-produced, part dimensions.

Technical Highlights

The highlights of the work this period fall into three areas. First, we established a cooperative working effort with AlliedSignal Ceramic Components (ASCC), as the work in this project is a joint effort between Argonne and ASCC. Second, we obtained the first three-dimensional (3-D), X-ray computed, tomographic image data for a gelcast M304 Teledyne-Continental (formerly Teledyne-Ryan Aeronautical) and demonstrated the initial detection sensitivity to voids in the lower part of the shaft where highest stresses are anticipated. Third, we obtained the first dimensional data sets for a complex turbine wheel, using both X-ray tomographic image data, as well as coordinate measuring machine (CMM) data, to be used to compare these two-dimensional data acquisition methods.

Technical Progress

NDE for Defect Detection

For detection of internal defects in a ceramic microturbine wheel, the initial approach we are taking is to use 3-D, high-spatial resolution, X-ray computed tomography (3D-XCT). In this period, the test specimen was an M304 gelcast wheel produced for Teledyne-Continental. The 3D-XCT scan was performed by obtaining a 720-projection data set using the X320 systems at a X-ray setup of 170 kVp/1.4 mA. The projection images were prefiltered with a 15-mil-thick lead sheet in order to remove beam hardening. The existing, cone-beam, reconstruction algorithm was used for 3-D image reconstruction.

Figure 1 presents horizontal and vertical reconstructions that show internal defects in the M304 turbine wheel near the lower end where high stresses are expected. The reconstructed images have a spatial resolution of 340 μm, and show that most of the cracks or pores are detected in the lower region of the turbine wheel.

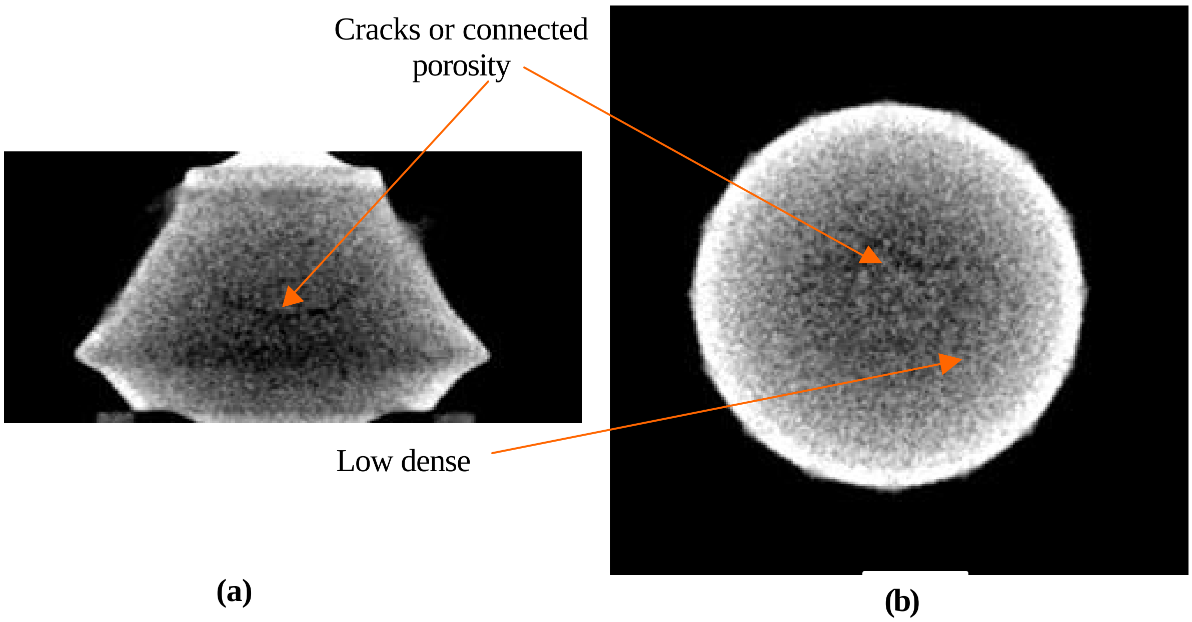

Figure 1. XCT reconstruction: (a) vertical reconstruction and (b) horizontal reconstruction.

NDE for Dimensional Measurements-Data Acquistion

The goal of this part of the work is to determine if NDE data can be used for fast, low-cost, dimensional data acquisition. For this work, edge detection is used to establish boundaries of an object using images from 3D-XCT-reconstructed data sets. During this period, an injection-molded, T-3 Si_3N_4 wheel was used which had been developed for automotive turbo-charger application. 3D- XCT were obtained on the rotor by utilizing the X-320 CT scanner at an X-ray setup of 170 kVp/1.4 mA. During the CT scan, 360 frames were captured over the entire viewing angle of 360 degrees and saved into a CT-scan file, which was used as input for the three-dimensional (3-D), cone-beam reconstruction. Each frame had a size of 450 x 180 pixels^2 with a spatial (pixel) resolution of 200 x 200 μm^2.

The approach used was to apply gray-scale threshold values on the reconstructed images. For the case presented in this report, the optimum threshold value was established by measuring the intensity of a pixel that had 50% of the maximum image contrast. As shown in Fig. 2-a, the image of the object edge was extracted from the original reconstructed image shown in Fig. 2-b by using a locally written algorithm. Figure 2-b, which is a superimposed image of the original reconstruction and the edge image, shows the accuracy of the edge-detecting method previously mentioned.

Turbine wheels, in general, have a symmetric core body with identical blades that are evenly located around the core body. This leads to consideration of the shape and position of blades. From the reconstruction data, the center of the rotor was determined and one blade was selected for use as a reference to develop the calculated/interpolated contour of each blade tip. The contours were expressed in terms of radius and angle, as

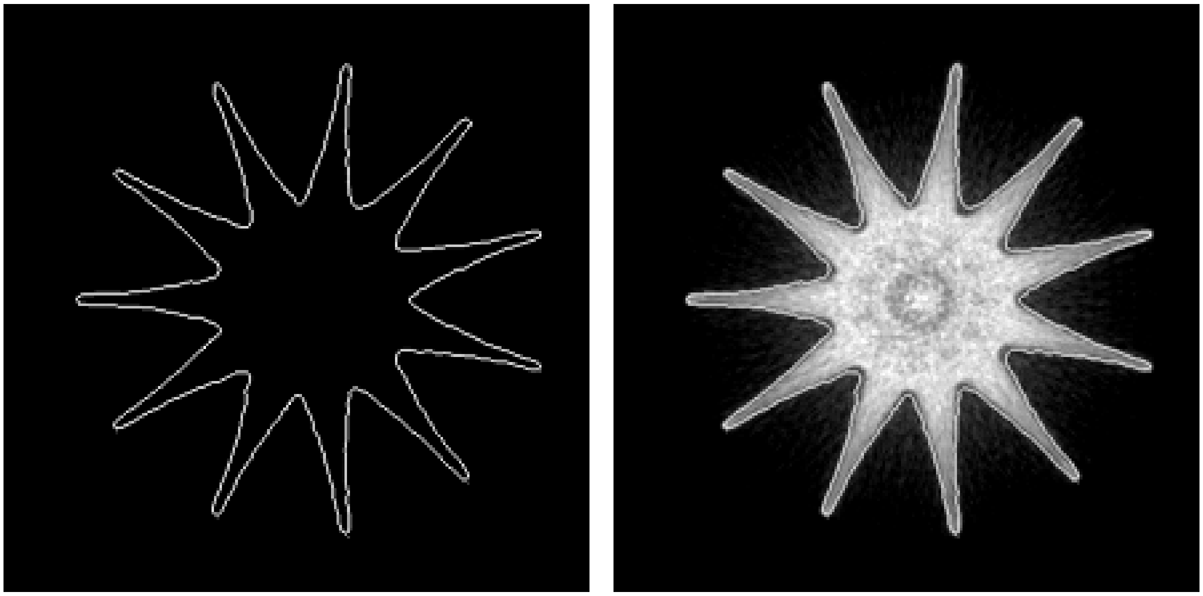

(a) **(b)**

Fig. 2. Accuracy of edge detecting method: (a) edge image of the reconstructed image shown in Fig. 2-b, and (b) superimposed image of the reconstructed image and its edge image of the reconstructed one.

seen in Equation 1which are third-order polynomials of z (i.e., vertical) position along the axis of rotation, where θ_o represents the angle of shift for each blade from the reference one. Four slices of reconstructions were selected for developing the polynomial functions for the contour of the reference blade. Figure 3 shows a point-cloud function of the microturbine, which includes the contours of blade-tips in 3-D space.

$$R(z) = a + bz + cz^2 + dz^3$$
$$\theta(z) = e + fz + gz^2 + hz^3 + \theta_o \quad (1)$$

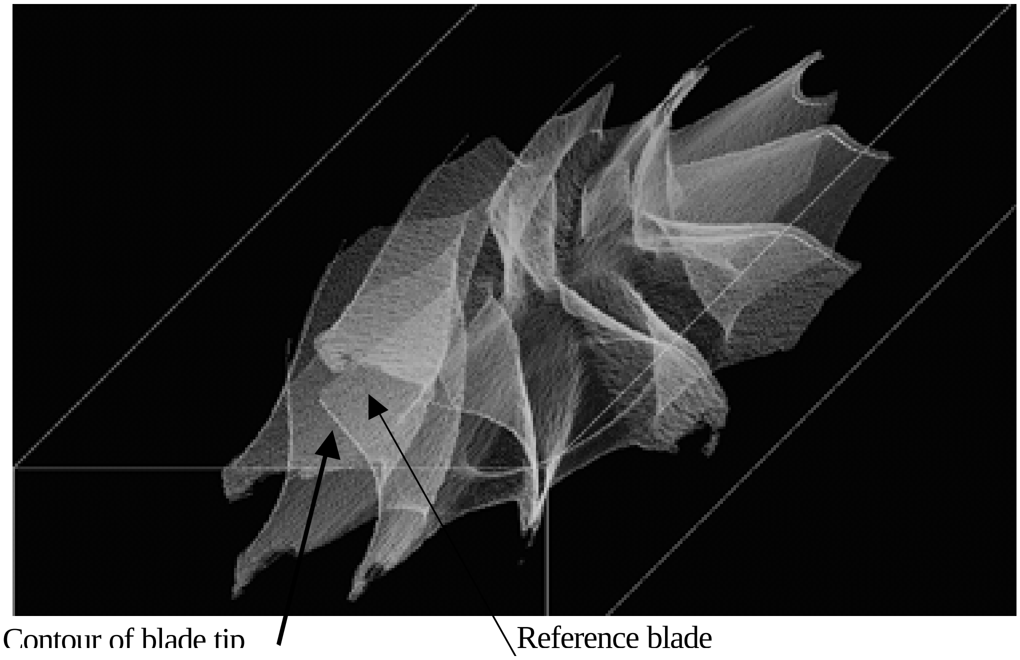

Figure 3. Point-cloud function with the contours of blade tips.

Comparison of 3DXCT and CMM data sets

To verify the feasibility of using 3D-XCT metrology, the 3D XCT data were compared to the most common method used for dimensional data, that is, CMM. The CMM method was used to generate one two-dimensional (2-D) edge image of the turbine rotor. The data acquisition took 4 h, because of the need to develop a procedure due to the complexity of the turbine rotor. The tolerance of this CMM measurement was determined to be ±0.5 mm in vertical direction and ±0.025 mm in horizontal direction. On the contrary, the 3D-XCT-image metrology shows ±0.2-mm tolerance in both directions, which corresponds to the spatial resolution of the reconstructed images and provides the entire 3-D, point-cloud function within <1 minute from the 3-D reconstructed image. Figure 4 shows the edge-detection images generated by both methods. In this report, the capability of the 3D-XCT and CMM methods for fast-dimensional analysis was compared. In the future, the accuracy of 3D-XCT metrology should be verified, which depends on various factors such as the number of projection due to the complexity and size of an object and the threshold value applied for development of an edge-detection image.

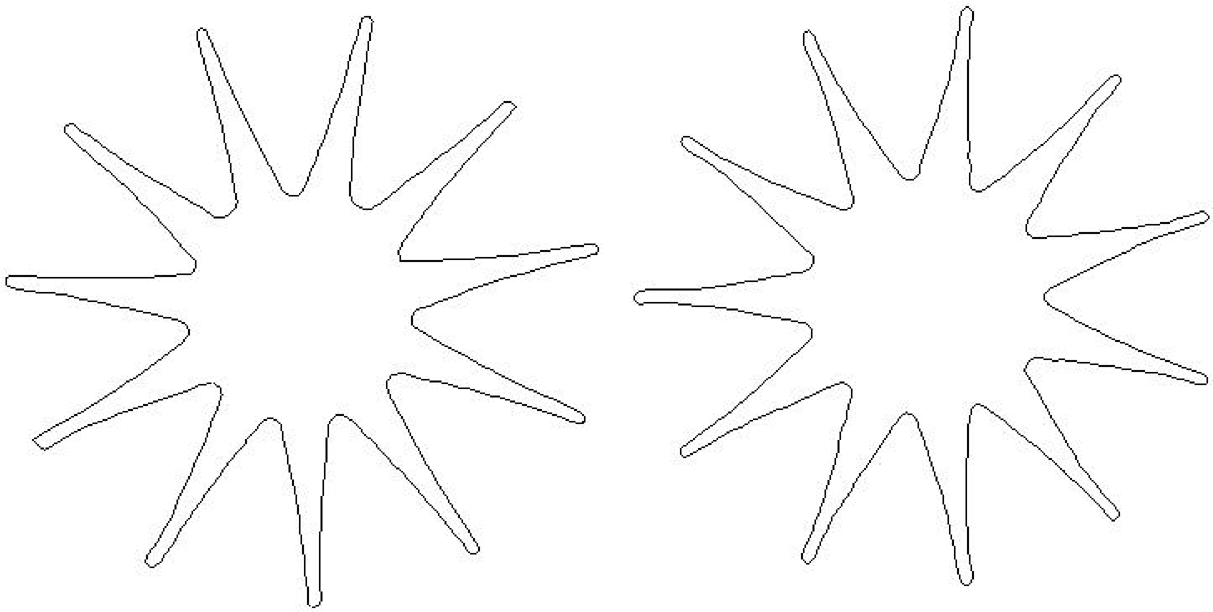

Fig. 4. Edge-detection images: (b) generated by CMM, and (a) generated by XCT-image metrology as shown in Fig 2-b.

Status of Milestones

All milestones are on schedule, since there was a delay getting this project started and a 2-month slippage was added to all milestones. The last milestone, milestone 3, is now underway.

Industry Interactions

There were several industrial interactions during this reporting period. These are listed in 3 topical areas: (1) microturbine manufacturers, (2) ceramic component suppliers, and (3) NDE technology related suppliers. In the case of microturbine suppliers, we had communication with (a) Capstone Corporation in Woodland Hills, CA, (b) Elliott Energy Systems in Stuart, FL, (c) Northern Research and Engineering Corporation of Woburn, MA, (d) AlliedSignal Power Systems of Phoenix, AZ, (e) Williams International of Walled Lake, MI, (f) Pratt & Whitney of East Hartford, CT, and (g) Solar Turbines of San Diego, CA. In the case of ceramic materials suppliers, we had communications with (a) AlliedSignal Ceramic Components of Torrance, CA and (b) Kyocera Industrial ceramics of Vancouver, WA. In the case of NDE related technologies, we had communications with (a) EG&G-Heimann Opto-Electronics of Wiesbaden, Germany, (b) EG&G Opto-electronics of Palo Alto, CA, and (c) V J Technologies of Long Island, NY, and (d) Hamamatsu of Bridgeater, NJ.

Problems encountered
None so far.

Publications
W. A. Ellingson and H. R. Lee, "Development of Metrological NDE Methods for Ceramic Components for Microturbines". Submitted to the 45th ASME Gas Turbine and Aeroengine Technical Congress and exposition, Munich, Germany, May 8-11, 2000

Life Prediction and Material Reliability Database for Ceramics

Noel Nemeth
NASA Glenn Research Center

Objective
Creation of a computerized database for selected ceramics for incorporation into analysis programs to predict component deformation and life. Also, enhancements to life prediction capabilities for arbitrary service load conditions incorporating aspects of probabilistic fatigue damage accumulation.

Highlights
A sample database for brittle material specimen rupture data was successfully developed using Microsoft Access and linked to a version of the CARES/Life code to enable Weibull and fatigue parameter estimation of data. The effort highlighted the potential, as well as exposed some of the weaknesses of the approach. Also, some early results from ongoing multi-axial creep experiments are shown.

Technical Progress
The integrated database with life prediction codes project is a new task element begun during FY'99. The purpose of this task is two-fold: first, to create an electronic database of representative specimen rupture data for brittle materials, and second, to integrate the materials database with life prediction codes such as CARES/Life for the purpose of assessing a material's Weibull and fatigue behavior. This project is distinct from internet-based, brittle material databases in that individual specimen rupture data will be recorded, as well as requisite Weibull and fatigue parameters unique to the reliability analysis code. This information will allow the design engineer to assess the pedigree of the source data as well as enable component level life prediction (reliability analysis). Currently, adoption and usage of probabilistic design codes is significantly hampered by the lack of availability of specimen rupture data for a representative spectrum of materials. The level of cooperation and integration that can be developed between the Glenn Research Center, The University of Dayton Research Institute, and Oak Ridge National Laboratory will be key to the ultimate success of the project.

The Microsoft Access database program was used for the first stages of this effort. Microsoft Access was chosen because of the ubiquity of the Microsoft Office software suite (Access is a component of Microsoft Office Professional Edition), as well as the fact that a royalty free Access runtime version can be freely distributed. Sample tables, forms, and queries were set up and made to interoperate using VBA (Visual Basic for Applications) code. A version of CARES/Life, in this case for the purpose in input file preparation which is FORTRAN-based, was made to work as a Windows DLL (Dynamic Link Library) in concert with the database. This work demonstrated the viability of linking a database program with an analysis code. The ability of Access to import Excel spreadsheet files as well as export and import of delimited text files was also demonstrated. This feature is useful for sharing data between separate database or website installations. On the negative side problems were encountered with update functions in a multi-user environment (even though there was only a single user) and getting fully successful database implementations on other computers with the Access runtime setup (mostly getting ActiveX controls to properly work). Also, incompatibilities in migrating from Office 97 to Office 2000 need to be resolved as well as issues of using the Jet Engine or MSDE (compatible with SQL Server 7.0) database formats within Access. These hurdles are not considered insurmountable, but they do add a level of annoyance to the project development.

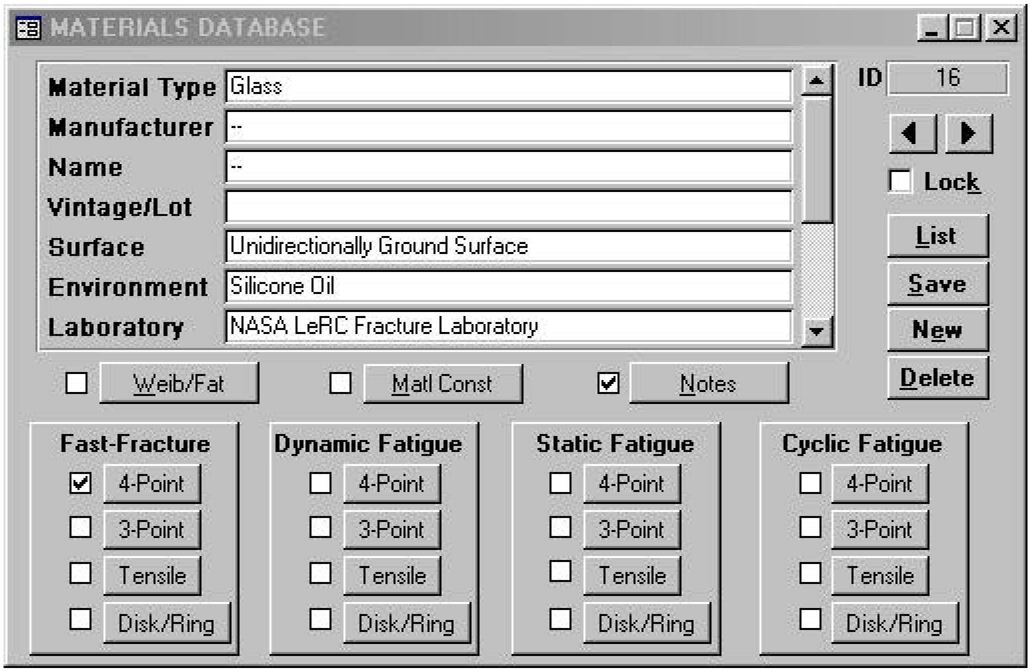

Figure 1. Sample form created in Access database.

Regarding data generation, extensive creep testing for NC 132 silicon nitride at 1300^{o}C in air is in progress using five different loading configurations such as pure tension, pure compression, uniaxial flexure, biaxial ring-on-ring flexure, and biaxial ball-on-ring flexure (see Fig. 2). The work is being undertaken with two primary objectives: the development of experimental techniques and the generation of creep database. Typical experimental data on creep deformation as a function of time for different loading configurations are shown in Fig. 3. Creep strain, creep parameters, basic creep mechanism, and other necessary information will be determined and analyzed for each loading configuration. This work will also be extended to predict creep behavior of a component subjected to multi-axial stress state, based on the pure tension and pure compression database generated.

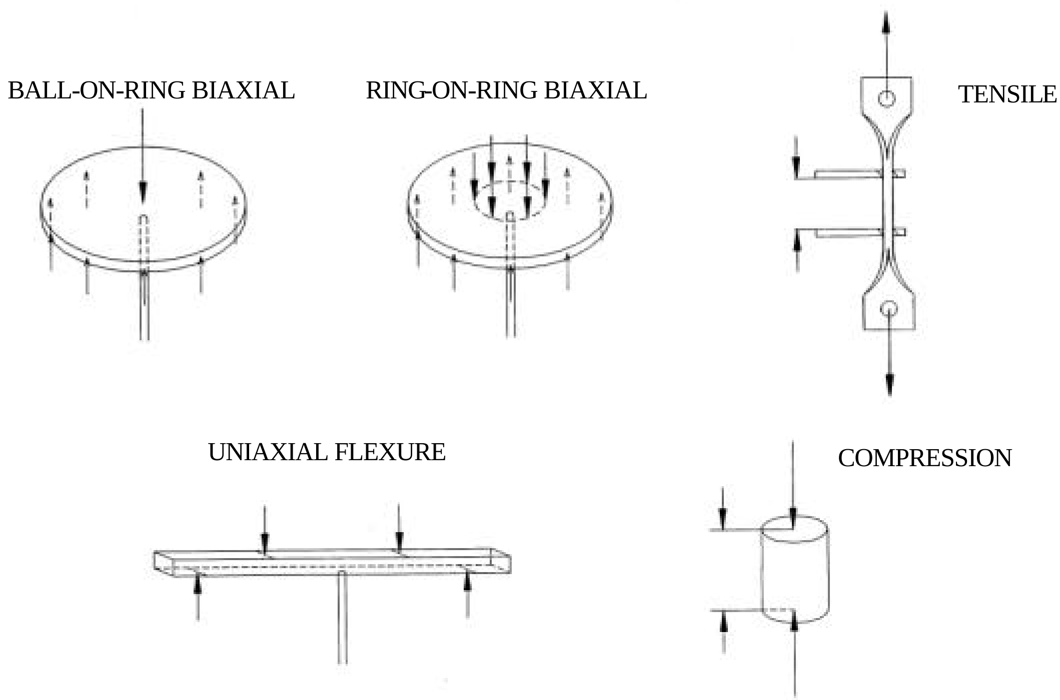

Figure 2. Experimental matrix for creep database for NC-132.

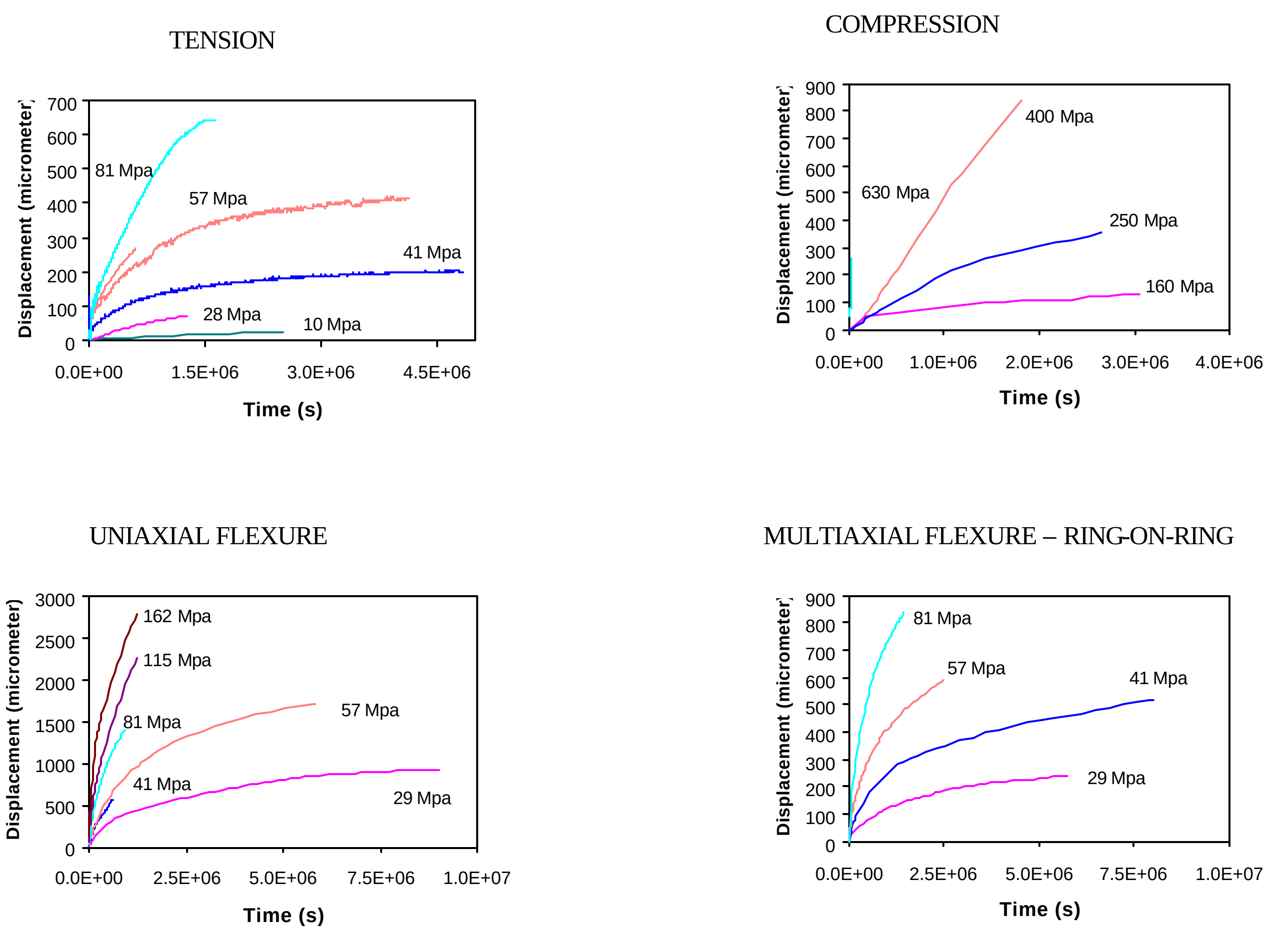

Figure 3. Database of NC132 silicon nitride under development.

Status of Milestones

On schedule.

Industry Interactions

None currently.

Problems Encountered

None significant.

Publications

“Elevated-Temperature, ‘Ultra’-Fast Fracture Strength of Advanced Ceramics: An Approach to Elevated-Temperature ‘Inet’ Strength”, S. R. Choi and J. P. Gyekenyesi, *ASME J. Eng. for Gas Turbines & Power*, Vol. 121, No. 1, pp. 18-24 (1999).

“Limitations in the Determination of Life Prediction Parameters of a Silicon Carbide with High
. R. Choi, *J. Mater. Sci. Lett*., Vol. 18, pp. 767-769 (1999).

“Slow Crack Growth Analysis of Brittle Materials with Finite Thickness Subjected to Constant Stress-Rate Testing,” S. R. Choi and J. P. Gyekenyesi, *J. Mater. Sci*., Vol. 34, pp. 3875-3882 (1999).

“’Ultra’-Fast Fracture Strength of Advanced Ceramics at Elevated Temperature,” S. R. Choi and J. P. Gyekenyesi, *Advances in Science & Technology* 13, pp. 675-682, Ed. P. Vincenzini, Techna Srl., Faenza, Italy (1999).

Internal Distribution

P. F. Becher, 4515, MS-6068, becherpf@ornl.gov
T. M. Besmann, 4515, MS-6063, besmanntm@ornl.gov
R. A. Bradley, 4508, MS-6161, bradleyra@ornl.gov
M. K. Ferber, 4515, MS-6069, ferbermk@ornl.gov
J. A. Haynes, 4515, MS-6063, haynesja@ornl.gov
D. R. Johnson, 4515, MS-6066, johnsondr@ornl.gov
M. A. Karnitz, 4515, MS-6065, karnitzma@ornl.gov
E. Lara-Curzio, 4515, MS-6069, laracurzioe@ornl.gov
R. J. Lauf, 4508, MS-6085, laufrj@ornl.gov
H. T. Lin, 4515, MS-6068, linh@ornl.gov
R. A. Lowden, 4515, MS-6063, lowdenra@ornl.gov
P. J. Maziasz, 4500S, MS-6115, maziaszpj@ornl.gov
K. L.. More, 4515, MS-6064, morekl1@ornl.gov
O. O. Omatete, 4508, MS-6087, atq@ornl.gov
B. A. Pint, 4500S, MS-6156, pintba@ornl.gov
A. C. Schaffhauser, 4500N, MS-6186, shaffhausac@ornl.gov
D. P. Stinton, 4515, MS-6063, stintondp@ornl.gov
R. W. Swindeman, 4500S, MS-6155, swindemanrw@ornl.gov
P. F. Tortorelli, 4500S, MS-6156, tortorellipf@ornl.gov
A. Wereszczak, 4515, MS-6069, wereszczakaa@ornl.gov
G. Wright, 4500S, MS-6157, wrightig@ornl.gov

External Distribution

ALLISON ADVANCED DEVELOPMENT CO., 1100 Wilson Blvd., Suite 1450, Arlington, VA 22209
J. Miles, r.jeffrey.miles@allison.com

ALM SYSTEMS, INC, 1920 N Street, NW, Suite 750, Washington, DC 20036
M. Kalin, mkalin@ibek.com

ARGONNE NATIONAL LABORATORY, 9700 S. Cass Ave., Argonne, IL 60439-4838
W. A. Ellingson, ellingson@anl.gov

BATTELLE COLUMBUS, 505 King Ave., Columbus, OH 43201
D. Anson

BAYSIDE MATERIALS TECHNOLOGY, 21150 New Hampshire Ave., Brookville, MD 20833
D. Freitag, dfreitag@ix.netcom.com

BCS, Inc., 5550 Sterrett Place, Suite 216, Columbia, MD 21044
D. Bartley, dbartley@bcs-hq.com

BOWMAN POWER
T. Davies, tdavies@bowman.power.demon.co.uk
T. Hynes, adh.bowmanpower@att.net

CALIFORNIA ENERGY COMMISSION
D. Hatfield, Dhatfiel@energy.state.ca.us

CANNON-MUSKEGON CORP., Box 506, Muskegon, MI 49443-0506
J. B. Wahl, jwahl@canmkg.com

CAPSTONE TURBINE CORP., 6430 Independence Ave., Woodland Hills, CA 91367
K. Duggan, kduggan@capstoneturbine.com
M. Stewart, mstewart@capstoneturbine.com

CATALYTICA COMBUSTION SYSTEMS, 430 Ferguson Dr., Mountain View, CA 94043
J. McCarty

CLEMSON UNIVERSITY, South Carolina Institute for Energy Studies, 386-2, Clemson, SC 29634-5180
L. P. Golan, glawren@clemson.edu

ELECTRIC POWER RESEARCH INSTITUTE, 3412 Hillview Ave., Palo Alto, CA 94303
J. Stringer, jstringe@epri.com

ELLIOTT ENERGY SYSTEMS, 2901 S.E. Monroe Street, Stuart, FL 34997
D. Burnham, dburnham@elliott-turbo.com

ENERGETICS, INC., 501 School St., SW, Suite 500, Washington, DC 20024
R. Scheer, rscheer@energeticsinc.com

ENERGY TECHNOLOGIES APPLICATIONS, 5064 Camino Vista Lujo, San Diego, CA 92130-2849
T. Bornemisza, borneger@ix.netcom.com

ENGINEERED CERAMICS, INC., 9617 Distribution Ave., San Diego, CA 92121
S. Limaye, slimaye@engceramics.com

STEVEN I. FREEDMAN, Engineering Consultant, 410 Carlisle Ave., Deerfield, IL 60015
S. I. Freedman, sifreedman@aol.com

GAS TURBINE ASSOCIATION, 1050 Thomas Jefferson St., NW, 5th Fl, Washington, DC 20007
J. Abboud, abboud@gasturbine.org

GENERAL ELECTRIC (GE) CR&D, 1 Research Circle, Building K1-RM 3B4, Niskayuna, NY 12309
S. Correa, correa@crd.ge.com
K. L. Luthra, luthra@crd.ge.com
J. M. VanDerwerken, vanderwerken@crd.ge.com

GENERAL ELECTRIC AIRCRAFT ENGINES, One Neumann Way, Mail Drop M89, Cincinnati, OH 45215-1988

R. Darolia, ram.darolia@ae.ge.com

GENERAL ELECTRIC POWER SYSTEMS, One River Rd., 55-127, Schenectady, NY 12345

R. Orenstein, robert.orenstein@ps.ge.com

HARRISON, ROBERT W., Materials and Processes Consultant, 4502 Longwood Court, Liberty Township, OH 45011-7236

R. W. Harrison, bobharrisonpe-fasm@worldnet.att.net

HOWMET RESEARCH CORP., 1500 South Warner St., Operhall Research Center, Whitehall, MI 49461-1895

B. Mueller, bmueller@howmet.com

R. Thompson, rthompson@howmet.com

HONEYWELL AEROSPACE, 1001 Pennsylvania Ave., N. W., Suite 7005, Washington, DC 46206-0420

H. Friedericy, Hans.Fredericy@honeywell.com

HONEYWELL CERAMIC COMPONENTS, 2525 W. 190th St., Torrance, CA 90504

D. Foley, dan.foley@honeywell.com
M. Gerstner, mary.gerstner@honeywell.com
D. Newson, danielle.newson@honeywell.com
J. Pollinger, john.pollinger@honeywell.com
M. Savitz, maxine.savitz@honeywell.com
D. Twait, doug.twait@honeywell.com
D. Wilson, dan.wilson@honeywell.com
J. Wimmer, jim.wimmer@honeywell.com

HONEYWELL COMPOSITES, 1300 Marrows Rd., PO Box 9559, Newark, DE 19714-9559

P. Craig, phil.craig@honeywell.com
K. Hatton, ken.hatton@honeywell.com
R. Matsumoto, roger.matsumoto@honeywell.com

HONEYWELL ENGINES, 2739 E. Washington St., PO Box 5227, Phoenix, AZ 85010

B. Schenk, bjoern.schenk@honeywell.com

HONEYWELL POWER SYSTEMS, 8725 Pan American Freeway NE, Albuquerque, NM 87113

K. Meister, kurt.meister@honeywell.com
H. A. Pursley, heidi.pursley@honeywell.com

KYOCERA INDUSTRIAL CERAMICS CORP., 5713 E 4th Plain Blvd., Vancouver, WA 98661

D. Carruthers, dave.carruthers@kyocera.com

NASA GLENN RESEARCH CENTER, 21000 Brookpark Rd., MS 49-7, Cleveland, OH 44135
D. Brewer, david.n.brewer@grc.nasa.gov
J. Gykenyesi, john.p.gyekenyesi@lerc.nasa.gov
S. Levine, stanley.r.levine@lerc.nasa.gov
N. Nemeth, noel.n.nemeth@grc.nasa.gov
B. Opila, Cleveland State Univ., MS 106-1, opila@grc.nasa.gov

NATIONAL RURAL ELECTRIC COOPERATIVE ASSOC., 4301 Wilson Blvd., SS9-204, Arlington, VA 22203-1860
E. Torrero, ed.torero@nreca.org

NATURAL RESOURCES CANADA, 1 Haanel Drive, Nepean, Ontario, Canada K1A 1M1
R. J. Brandon, rbrandon@NRCan.gc.ca

NREC, 39 Olympia Ave., Woburn, MA 01801-2073
P. Baldwin, spb@nrec.com

NREC, 32 Exeter St., Portsmouth, NH 03801
J. Johnson, jtj@nrec.com
J. Kesseli, jbk@nrec.com

NYSERDA, Corporate Plaza West, 286 Washington Avenue Extension, Albany, NY 12203-6399
R. Drake, rld@mailgate.nyserda.org

ONTARIO POWER GENERATION, 800 Kipling Avenue, Room KR286, Toronto, Canada M8Z 6C4
N. Jagan Nicholas.Jagan@oht.hydro.on.ca

PCC AIRFOILS, INC., 25201 Chagrin Blvd., Suite 290, Beachwood, OH 44122
C. Kortovich, graham@hp750.pccairfoils.com

PENN STATE UNIVERSITY, Applied Research Laboratory, PO Box 30, State College, PA 16823
J. Singh, jxs46@psu.edu

PRATT & WHITNEY, PO Box 109600, MS-706-06, West Palm Beach, FL 33410-9600
G. Linsey, linseygd@pwfl.com

PRAXAIR SURFACE TECHNOLOGIES, 1500 Polco St., Indianapolis, IN 46224
R. C. Novak, richard_c_novak@praxair.com

RENSSELAER POLYTECHNIC INSTITUTE, Mechanical Engineering, 110 8th St., Troy, NY 12180-3590
B. Thompson, Thompson@rpi.edu

RICHERSON AND ASSOC., 2093 E. Delmont Dr., Salt Lake City, UT 84117
D. Richerson, RichersonD@aol.com

ROLLS-ROYCE ALLISON, 2925 W. Minnesota St., PO Box 420, Indianapolis, IN 46241
S. A. Ali
S. Berenyi
P. Heitman, peter.w.heitman@allison.com
F. Macri, francis.g.macri@allison.com
R. Wenglarz, richard.a.wenglarz@allison.com

SEBESTYEN, T., Consultant, 1309 Park Garden Lane, Reston, VA 20194-1998
sebestyen@email.msn.com

SIEMENS WESTINGHOUSE POWER CORP., 1310 Beulah Rd., Pittsburgh, PA 15235-5098
M. A. Burke, michael.burke@swpc.siemens.com
C. Forbes, christian.forbes@swpc.siemens.com

SOLAR TURBINES, INC., TurboFab Facility, 16504 DeZavala Rd., Channelview, TX 77530
B. Harkins

SOLAR TURBINES INC., 818 Connecticut Ave., NW, Suite 600, Washington, DC 20006-2702
R. Brent, solardc@bellatlantic.net

SOLAR TURBINES, INC., 2200 Pacific Highway, PO Box 85376, MZ R, San Diego, CA 92186-5376
P. Browning, Browning_Paul_F@solarturbines.com
M. Fitzpatrick, Fitzpatrick_mike_d@solarturbines.com
M Van Roode, van_roode_mark@solarturbines.com
M. Ward, Ward_Mike_E@solarturbines.com

SOUTHERN CALIFORNIA EDISON COMPANY, 2244 Walnut Grove Avenue, Rosemead, CA 91770
S. Hamilton, hamiltsl@sce.com

TELEDYNE CONTINENTAL MOTORS, 1330 W. Laskey Rd., PO Box 6971, Toledo, OH 43612-0971
J. T. Exley, texley@teledyne.com

UCI COMBUSTION LABORATORY, U. of CA, Irvine, Irvine, CA 92697-3550
V. McDonell, mcdonell@ucicl.uci.edu

UDRI, Ceramic & Glass Laboratories, 300 College Park Ave., Dayton, OH 45469-0172
G. Graves, gravesga@udri.udayton.edu
N. Osborne, Osborne@udri.udayton.edu

UNITED TECHNOLOGIES, 400 Main St., MS 165-22, East Hartford, CT 06108
W. Day, dayw@pweh.com

UNITED TECHNOLOGIES RESEARCH CENTER, 411 Silver Lane MS 129-24, East Hartford, CT 06108
F. Biancardi biancafr@utrc.utc.com
H. E. Eaton, eatonhe@utrc.utc.com
J. Holowczak, holocje@utrc.utc.com
J. Smeggil, smeggiljg@utrc.utc.com

UNIVERSITY OF CALIFORNIA, Department of Mechanical Engineering, Berkeley, CA 94720
R. Dibble, rdibble@newton.berkeley.edu

U.S. ADVANCED CERAMICS ASSOCIATION (USACA), 1600 Wilson Blvd., Suite 1008, Arlington, VA 22209
B. Werst, wwerst@advancedceramics.org

US DOE-FETC, P. O. Box 880, MSO-D01, 3610 Collins Ferry Rd., Morgantown, WV 26507-0880
C. Alsup, Jr., charles.alsup@fetc.doe.gov
A. Layne, abbie.layne@fetc.doe.gov

US DOE-FETC, PO Box 10940, Pittsburgh, PA 15236
M. Mathur, mathur@fetce.doe.gov
U. S. Rao, rao@fetc.doe.gov

US DOE CHICAGO OPERATIONS OFFICE, 9800 S. Cass Ave., Argonne, IL 60439
J. E. Jonkouski, jilljonkouski@ch.doe.gov
J. Mavec, joseph.mavec@ch.doe.gov
J. Livengood, joanna.livengood@ch.doe.gov
S. Waslo, Stephen.waslo@ch.doe.gov

US DOE-HQ, 1000 Independence Ave., S.W., Washington DC 20585
D. Haught, debbie.haught@ee.doe.gov
P. Hoffman, patricia.hoffman@ee.doe.gov
H. Kerch
T. King, Tom.King@ee.doe.gov
W. P. Parks, william.parks@ee.doe.gov
S. L. Richlen, Scott.Richlen@hq.doe.gov
M. Smith, merrill.smith@ee.doe.gov
C. A. Sorrell, charles.sorrell@ee.doe.gov

WILLIAMS INTERNATIONAL, 2280 West Maple Rd., PO Box 200, Walled Lake, MI 48390-0200
R. Oates, roates@williamks-int.com
C. Schiller, cschiller@williams-int.com